UNCLASSIFIED
Security Classification

DOCUMENT CONTROL DATA - R & D
(Security classification of title, body of abstract and indexing annotation must be entered when the overall report is classified)

1. ORIGINATING ACTIVITY (Corporate author)
IIT Research Institute
10 West 35th Street
Chicago, Illinois 60616

2a. REPORT SECURITY CLASSIFICATION
Unclassified

2b. GROUP

3. REPORT TITLE
Submicron Separation and Data

4. DESCRIPTIVE NOTES (Type of report and inclusive dates)
Task II (1) Subtask B, November 1, 1971 through May 31, 1972

5. AUTHOR(S) (First name, middle initial, last name)
Walter J. Wnek
Reg Davies

6. REPORT DATE	7a. TOTAL NO. OF PAGES	7b. NO. OF REFS
May 1972	101	44

8a. CONTRACT OR GRANT NO.	9a. ORIGINATOR'S REPORT NUMBER(S)
F33657-71-C-0859	IITRI-C6239-A005-3
b. PROJECT NO. VT/1414/RDE/ASD	
c. ARPA Order No. 1702	9b. OTHER REPORT NO(S) (Any other numbers that may be assigned this report)
d. Program Code No. 1F10	

10. DISTRIBUTION STATEMENT
This [illegible]

11. SUPPLEMENTARY NOTES

12. SPONSORING MILITARY ACTIVITY
AFTAC/NYRC
Alexandria, Virginia

13. ABSTRACT

The present theory for predicting the dependence of the force of adhesion on zeta potential, surface charge, electrolyte or surfactant concentration and pH is reviewed. It is shown to be inadequate for explaining experimental observations. New theory is developed which explains these observations and is in good quantitative agreement with experimental data in the literature.

DD FORM 1 NOV 68 1473

UNCLASSIFIED
Security Classification

DISCLAIMER NOTICE

THIS DOCUMENT IS THE BEST QUALITY AVAILABLE.

COPY FURNISHED CONTAINED A SIGNIFICANT NUMBER OF PAGES WHICH DO NOT REPRODUCE LEGIBLY.

14. KEY WORDS	LINK A		LINK B		LINK C	
	ROLE	WT	ROLE	WT	ROLE	WT
Adhesion						
Agglomeration						
Submicron Particles						
van der Waals forces						
Suspensions						
Dispersion						
Size Distribution						
Zeta Potential						
pH						
Surface Energy						
Surface Charge						
Surfactant Concentration						
Electrolyte Concentration						

FOREWORD

This report is submitted to HQ U.S.A.F. (AFTAC/NYRC) as the Final Report on Task II (1) Subtask B entitled "Extension and Development of Theoretical Models." Significant progress has been made during the performance of this task, resulting in a highly effective model to enable the optimum conditions for submicron particle separation to be predicted.

Prepared by

Walter J. Wnek
Associate Chemical Engineer
Chemical Engineering Research

Reg Davies
Senior Physicist
Fine Particle Research

Approved by

John Stockham
Manager
Fine Particle Research

WJW:nr

ABSTRACT

The present theory for predicting the dependence of the zeta potential and surface charge of colloidal particles on the concentration of electrolytes, surfactants, and pH is reviewed and shown to be inadequate for explaining experimental observations. A new theory is developed which explains these observations and is in good quantitative agreement with experimental data in the literature.

This theory considers the various ways in which a surface charge can develop on a particle. These include adsorption of complex ions derived from electrolytes and from the particle itself and dissociation of surface groups due to chemical reactions at the particle surface. Adsorption isotherms are developed for each case. Since the surface charge and potential enter into the expressions for these isotherms, the relationship between the zeta potential, surface potential and surface charge is investigated. The result is an analytical expression for planar surfaces and a computer program for spherical surfaces. When the adsorption isotherms are used in combination with these results, the manner in which the zeta potential and surface charge depend on ionic strength, surfactant concentration and pH is completely described.

The theory is compared with experimental data available in the literature and good agreement between them is found. A computer program was developed to perform the regression analysis required for estimating the adsorption energies and number of adsorption sites which are the parameters in the theory.

The theory for the interaction energy between two particles is also investigated. It is concluded that the theory for van der Waals-London forces is sufficiently complete so that no improvements are needed. However, in case of the electrical

forces arising from double layer interaction, the present theory is extended to obtain approximate analytical expressions which give this interaction energy for arbitrary surface potentials, particle size, and separation distance. Approximations available in the literature are restricted to either particles at the same potential or to potentials smaller than 50 mv. Although exact numerical calculations have been performed, the results are in tabular form and are inconvenient to use. Since the interaction energy curve is to be used later in the program in further integrations, it is necessary to have analytical expressions to avoid unwielding numerical problems.

TABLE OF CONTENTS

TABLE OF CONTENTS (cont.)

LIST OF TABLES AND FIGURES

LIST OF TABLES AND FIGURES (cont.)

1. INTRODUCTION

As motivation for why the work to be presented was performed, two unexplained experimental observations which are commonly encountered in the study of the stability of colloidal systems will be discussed. Then, the present theory available for interpreting colloidal phenomena will be reviewed, and it will be shown that it is unable to account for these experimental results.

The most typical kind of data that can be obtained for characterizing a colloidal system is the zeta potential versus concentration curve as shown in Figure 1 for the colloid minusil in various electrolytic solutions. The reason why this curve is of importance is that it gives the electric potential at the surface of a colloidal particle from which is calculated the force, or more properly, the energy of interaction between two particles as they approach each other. If the particles have the same surface potential, a curve representing the repulsion energy versus separation between the particles is obtained as shown in Figure 2. When this curve is combined with the attraction curve due to van der Waals or London forces, the total interaction energy versus separation curve as shown in Figure 2 is obtained whose maximum represents the energy barrier which the particles must overcome in order to make lasting contact. Since the repulsion curve depends on the value of the surface potential, the zeta potential determines the magnitude of the energy barrier. Values of the zeta potential around zero indicate an unstable system while large positive or negative values suggest stability.

For the case of the phosphate $Na_4P_2O_7$ examination of Figure 1 shows that as the concentration is increased, the zeta potential initially becomes more negative but gradually levels off and then becomes less negative until it reaches zero whereupon it would no longer change with concentration. Similar

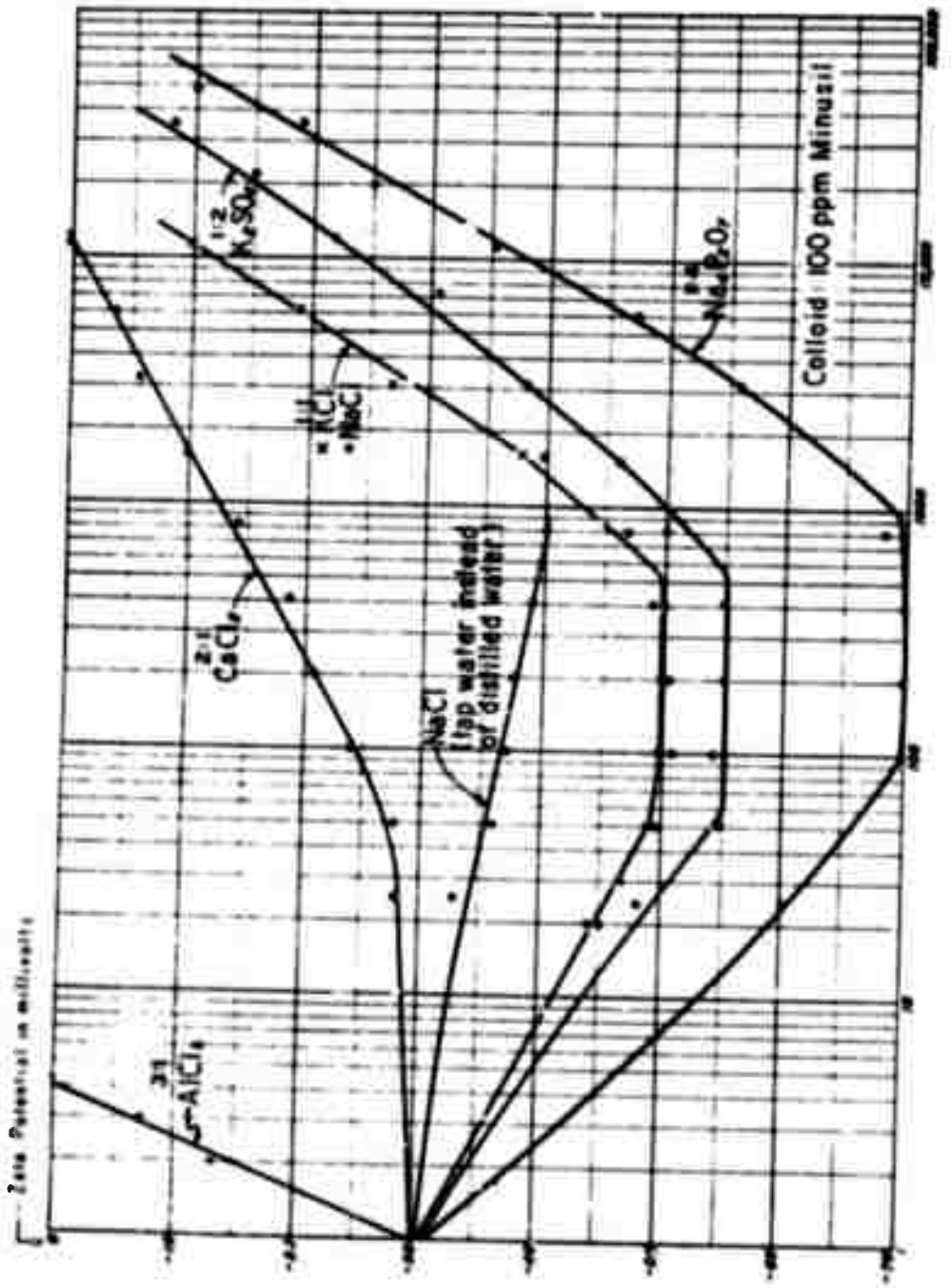

Figure 1

CONCENTRATION OF ELECTROLYTE - PPM
(from Riddick, 1968)

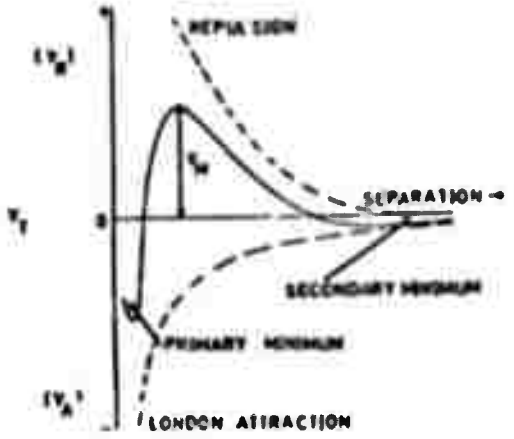

Figure 2

TOTAL POTENTIAL ENERGY (V_T) DIAGRAM
FOR TWO COLLOIDAL PARTICLES
(from Napper, 1970)

results are obtained for KCl, NaCl, and K_2SO_4. However, in the case of $AlCl_3$ and $CaCl_2$, it is seen that the zeta potential initially becomes less negative upon increasing the concentration. If the curves for $AlCl_3$ and $CaCl_2$ were continued to higher concentrations, it would be found that the zeta potential would cross zero and become more and more positive until it would reach a maximum after which it would steadily decrease to zero and no longer change with concentration. It is interesting to note from such data that the same electrolyte can stabilize or agglomerate a colloidal system depending on its concentration.

The second curious observation arises from experiments in which the adsorption density of ions adsorbed onto a surface and thus the surface charge is measured for various concentrations of an indifferent or nonadsorbing electrolyte. Figure 3 shows such curves as determined for ferric oxide where the adsorption density of hydrogen and hydroxide ions is given as a function of pH and ionic strength. Similarly, Figure 4 gives the surface

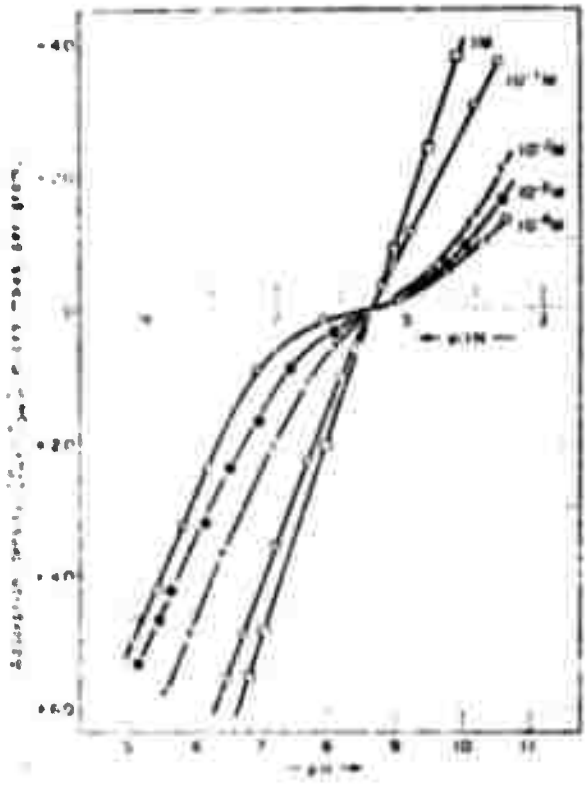

Figure 3

ADSORPTION DENSITY OF POTENTIAL DETERMINING IONS ON FERRIC OXIDE AS A FUNCTION OF pH AND IONIC STRENGTH: TEMPERATURE, 21°C; INDIFFERENT ELECTROLYTE KNO_3 (from Parks and de Bruyn, 1962)

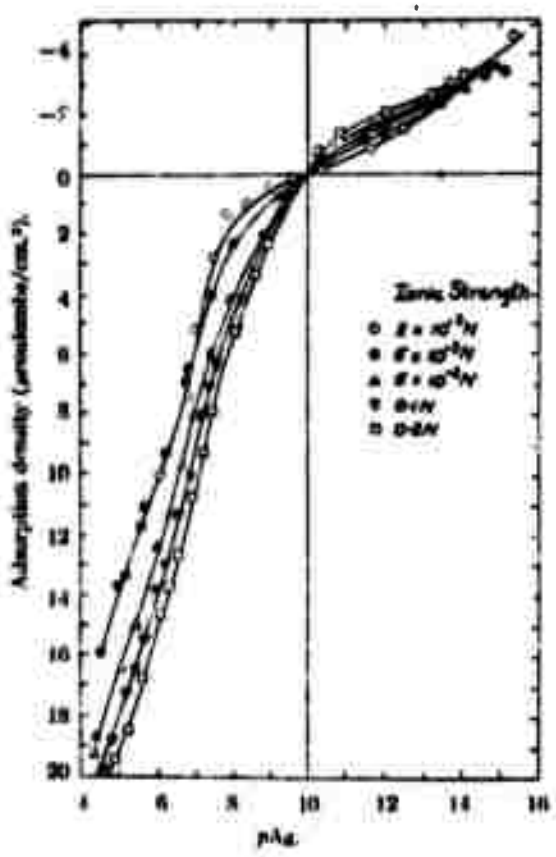

Figure 4

ADSORPTION DENSITY OF POTENTIAL DETERMINING IONS
ON SILVER SULFIDE AS A FUNCTION OF THE pAg
(from Freyberger and de Bruyn, 1957)

charge on silver sulfide as function of pAg and ionic strength, and Figure 5 the charge on alumina as a function of pH and ionic strength. The observation to be explained here is that if the surface is positively charged, an increase in ionic strength makes the adsorption density or surface charge more positive. However, if the surface is negatively charged, an increase in ionic strength makes the adsorption density and surface charge more negative. Also, the point where the surface charge becomes zero is independent of ionic strength. Since the zeta potential depends on both surface charge and ionic strength, it is necessary to explain this observation in conjunction with the previous one in order to obtain a good understanding of the zeta potential-concentration relationship.

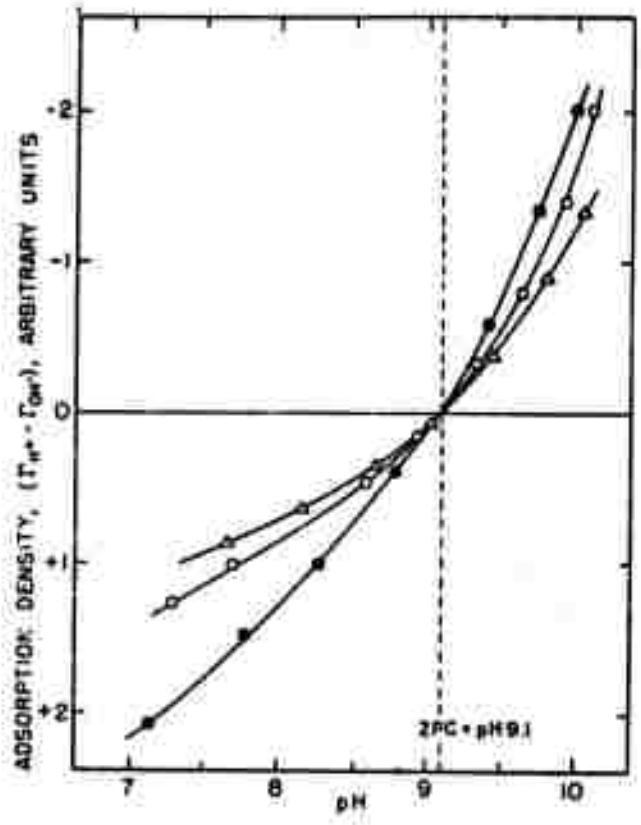

Figure 5

ADSORPTION DENSITY OF POTENTIAL-DETERMINING IONS ON ALUMINA AT 25.0°C AS A FUNCTION OF pH AND IONIC STRENGTH, USING KCl AS SUPPORTING ELECTROLYTE
KCl, NORMALITY: △ —— 10^{-3}; ○ —— 10^{-2}; ● —— 10^{-1}
(from Yopps and Fuerstenau, 1964)

2. PRESENT THEORY

The present theory available for analyzing these phenomena is the Gouy-Stern-Grahame model of the electrical double layer (Parfitt, 1969). As shown in Figure 6, the double layer is divided into three parts: (1) the region next to the solid surface contains ions adsorbed onto the surface, (2) the second region takes into account the fact that counter ions which are not adsorbed but are attracted to the surface due to electrostatics cannot approach the surface closer than some distance due to their finite size, and (3) the third part is the diffuse layer as determined by the Poisson-Boltzmann equation.

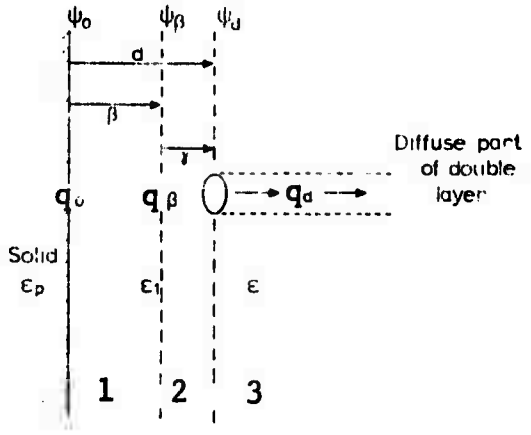

Figure 6

MODEL FOR THE ELECTRIC DOUBLE LAYER AT THE SOLID-SOLUTION INTERFACE SHOWING POTENTIALS ψ AND CHARGE DENSITIES q (from Parfitt, 1969)

From the condition that the system be electrically neutral

$$q_0 + q_\beta + q_d = 0 \qquad (1)$$

where q denotes charge per unit area.

Defining the total capacity of the two inner regions as

$$C = \frac{\epsilon_1}{4\pi d}$$

where ϵ is the dielectric constant then

$$C_1 = \frac{d}{\beta} C$$

$$C_2 = \frac{d}{\gamma} C$$

From the definition of capacity, one may write

$$\frac{\psi_0 - \psi_\beta}{\sigma_0} = \frac{1}{C_1} = \frac{\beta}{Cd} \qquad (2)$$

and

$$\frac{\psi_\beta - \psi_d}{\sigma_0 + \sigma_\beta} = \frac{1}{C_2} = \frac{\gamma}{Cd} \qquad (3)$$

where ψ is electric potential. The classical Gouy-Chapman equation is used to relate q_d and ψ_d

$$q_d = -\sqrt{\frac{2\epsilon RTc}{1000\,\pi}} \quad \text{Sinh} \frac{ze\psi_d}{kT} \qquad (4)$$

where

R is the universal gas constant

k is Boltzmann constant

T is absolute temperature

z is valence

e is charge of an electron

c is molarity of electroyte in the bulk solution

The Stern adsorption isotherm is then introduced in order to relate the surface charge due to adsorption to the bulk concentration

$$q_\beta = \frac{zeN_0Mc}{1000} \exp\left[-\frac{ze\psi_\beta + \Phi}{kT}\right] \qquad (5)$$

where

N_0 is the number of adsorption sites per unit area

M is molecular weight of dispersion medium

Φ is the energy of adsorption

Finally, the surface potential is related to the bulk concentration by the thermodynamic relationship

$$\psi_0 = \frac{kT}{e} \ln \frac{c}{c_{zpc}} \qquad (6)$$

where c_{zpc} is the bulk concentration for which the surface charge is zero.

It is of interest to list the parameters which are not known in the Gouy-Stern-Grahame model. The capacities and thicknesses of regions 1 and 2 contribute the four parameters C_1, C_2, β and α while the Stern equation contributes the two parameters Φ and N_0. One would expect that with six arbitrary constants, it would be possible to fit this model easily to zeta potential versus concentration data by judicious selection of the values of these constants. However, Hunter and Wright (1971) have found that this is not necessarily true and had difficulty in obtaining agreement between the Gouy-Stern-Grahame theory and data when they tried to apply it to several sets of data available in the literature. In many cases, agreement could only be

obtained when somewhat unreasonable values of the various parameters were used, and unrealistic assumptions were made. For example, for alumina, it was necessary to postulate adsorption of Na^+ and Cl^- ions onto positively and negatively charged surfaces, respectively. Such a phenomenon is known not to occur to any great extent if at all. These investigators came to the conclusion that the Gouy-Stern-Grahame model is inadequate to describe satisfactorily the concentration dependence of the zeta potential and that a more sophisticated model is needed.

In the sections that follow, such a model is presented. The papers (see References) of Ottewill and his students, Parks, and Stumm and Morgan were of great assistance in developing the concept of this model and formed the foundations of the theoretical work. It is shown that this model easily explains the experimental observations previously discussed as well as others and is in quantitative agreement with data. The reason why this model is more successful in describing the concentration dependence of the zeta potential than was the Gouy-Stern-Grahame model is that more physics was incorporated into the model. As a result, nebulous quantities such as the capacities of the inner regions did not have to be introduced in the model so that all the parameters are of a fundamental and basic nature.

3. SURFACE CHARGE DUE TO MULTI-COMPONENT ADSORPTION FROM SOLUTION ONTO A SOLID

Surface charge on a solid particle can be established by the adsorption of ions from solution. Preferential adsorption of one species over another can result from electrostatic attraction, London-van der Waals interaction, hydrogen bonding, and chemical reactions at the surface. For example, cationic polyelectrolytes adsorb on negatively charged particles by electrostatic attraction and non-ionic and anionic ones by van der Waals attraction and hydrogen bonding despite the electrostatic repulsion in the case of the anionic polymer. Polynuclear hydroxometal complexes and phosphates adsorb onto oxide surfaces by chemical surface reactions. In the sections that follow, these adsorption mechanisms will be discussed, and expressions for the adsorption isotherms will be derived.

Under the assumption that adsorption of species in solution occurs on independent localized sites on the surfaces of a solid, it has been shown (Fowler and Guggenheim, 1965) that in accordance with the methods of statistical mechanics, the chemical potential μ_i of each adsorbed species i from solution onto a solid surface may be written as

$$\mu_i = \mu_i^A + kT \ln \left\{ \frac{\theta_i}{1 - \sum_j \theta_j} \right\} \qquad (7)$$

where

μ_i^A is the chemical potential of the i^{th} species on the solid at the standard state defined as half coverage of the surface by the i^{th} species or $\theta_i = 0.5$

k is Boltzmann constant

T is absolute temperature

θ_i is the fraction of available sites occupied by the i^{th} species.

From classical thermodynamics, the chemical potential of the i^{th} species in the bulk solution is given by

$$\mu_i = \mu_i^s + kT \ln \nu_i x_i \tag{8}$$

where

μ_i^s is the chemical potential of the i^{th} species in solution at the standard state defined as unit activity of the i^{th} species

x_i is the mole fraction of the i^{th} species in solution

ν_i is its activity coefficient.

At equilibrium, the chemical potential of the i^{th} species must be the same in both the solid and liquid phases. Thus, Equations 7 and 8 may be equated to each other to give

$$\frac{\theta_i/\nu_i x_i}{1 - \sum_j \theta_j} = \exp\left[-\frac{\Delta G_i^0}{kT}\right] \tag{9}$$

where $\Delta G_i^0 = \mu_i^A - \mu_i^s$ and is the overall standard free energy of adsorption. This term consists of the sum of the specific physical or chemical adsorption energy and the electrostatic work involved in transporting an ion from the bulk solution to the charged surface and can be written as

$$\Delta G_i^0 = \Phi_i + z_i e \psi_0$$

where

Φ is the energy per ion of specific adsorption due to nonelectrostatic forces

ψ_0 is the electrical potential at the surface.

The electrostatic term is obtained as follows. The work W required to transport a charge q in an electric field of strength E from the bulk to the surface is

$$W = -\int_{\infty}^{0} Eq\,dx = \int_{\infty}^{0} q\,\frac{d\psi}{dx}\,dx = q\psi_0$$

Since this work is per ion, $q = ze$ and $W = ze\psi_0$.

If n_i is the number of molecules if the i^{th} species adsorbed and N_i the number of adsorption sites available for it, then

$$\theta_i = \frac{n_i}{N_i} \tag{10}$$

so that Equation 9 becomes

$$n_i = \nu_i x_i N_i \left[1 - \sum_j \frac{n_j}{N_j}\right] b_i \tag{11}$$

where for simplicity the term

$$b_i = \exp\left[-\frac{\Delta G_i^0}{kT}\right]$$

has been introduced. Equation 11 defines a system of coupled equations in the unknowns n_j. Fortunately, if the ratio of Equation 11 for two different values of i is taken, n_j can be expressed in terms of n_i as

$$n_j = \frac{\nu_j x_j N_j b_j}{\nu_i x_i N_i b_i}\, n_i \tag{12}$$

Then, substituting Equation 12 into 11,

$$n_i = \nu_i x_i N_i b_i - n_i \sum_j \nu_j x_j b_j$$

or solving for n_i

$$n_i = \frac{\nu_i x_i N_i b_i}{1 + \sum_j \nu_j x_j b_j} \tag{13}$$

Thus, in this way it has been possible to decouple Equation 11 and solve explicitly for each n_i in terms of only ν_j, x_j, b_j, and N_i.

The total charge q on the surface of the solid can now be determined by summing the contributions of each species

$$q = \sum_i z_i e n_i \tag{14}$$

where

z_i is the valence of the i^{th} species

e is the charge of an electron (1.6×10^{-19} coul).

Substituting Equation 13 into 14, the expression for the charge becomes

$$q = \sum_i \frac{z_i e N_i \nu_i x_i b_i}{1 + \sum_j \nu_j x_j b_j} \tag{15}$$

Equation 15 is a multi-component version of the Langmuir adsorption isotherm.

It is also possible for the various species to adsorb not only on the solid but also onto each other so that multi-layer adsorption can occur. By analogy with Equation 13, the number of molecules of the i^{th} species which are adsorbed onto molecules of the m^{th} species already on the solid can be written as

$$n_{im} = \frac{\nu_i x_i n_m b_{im}}{1 + \sum_j \nu_j x_j b_{jm}} \tag{16}$$

by considering n_m as the number of available sites for formation of a second adsorption layer. The notation for the subscript "im" refers to the i^{th} species adsorbed onto the m^{th} species on the solid. The additional charge on the solid due to this second adsorption layer is

$$\Delta q = \sum_m \sum_k z_{km} e n_{km} \tag{17}$$

or substituting Equation 16 into 17

$$\Delta q = \sum_m \sum_k \frac{z_{km} e \nu_k x_k n_m b_{km}}{1 + \sum_j \nu_j x_j b_{jm}} \tag{18}$$

Then substituting Equation 13 into 18

$$\Delta q = \sum_m \sum_k \frac{z_{km} e \nu_k x_k b_{km}}{1 + \sum_j \nu_j x_j b_{jm}} \cdot \frac{\nu_m x_m N_m b_m}{1 + \sum_j \nu_j x_j b_j}$$

or

$$\Delta q = \frac{e}{1 + \sum_j \nu_j x_j b_j} \sum_m \frac{\nu_m x_m N_m b_m}{1 + \sum_j \nu_j x_j b_{jm}} \sum_k z_{km} \nu_k x_k b_{km} \tag{19}$$

For the case where each species adsorbs only onto species of the same kind, then

$$b_{km} = \begin{cases} 0 & \text{if } k \neq m \\ b_{mm} & \text{if } k = m \end{cases}$$

Thus, Equation 19 becomes

$$\Delta q = \frac{1}{1 + \sum_j \nu_j x_j b_j} \sum_m z_m e \nu_m x_m N_m b_m \cdot \frac{\nu_m x_m b_{mm}}{1 + \nu_m x_m b_{mm}} \qquad (20)$$

If the charges due to the first and second adsorption layers as given by Equations 15 and 20 are combined, the expression for the total charge on the solid is

$$q_T = \frac{1}{1 + \sum_j \nu_j x_j b_j} \sum_i z_i e N_i \nu_i x_i b_i \left[1 + \frac{\nu_i x_i b_{ii}}{1 + \nu_i x_i b_{ii}} \right] \qquad (21)$$

In the case where each species has access to the same available sites so that $N_i = N_0$, then Equation 21 becomes

$$q_T = \frac{N_0 e}{1 + \sum_j \nu_j x_j b_j} \sum_i z_i \nu_i x_i b_i \left[1 + \frac{\nu_i x_i b_{ii}}{1 + \nu_i x_i b_{ii}} \right] \qquad (22)$$

If N_0 is expressed as number of sites per unit area, the the units of the charge is coulombs per unit area.

4. THE RELATIONSHIP BETWEEN SURFACE CHARGE AND THE ZETA POTENTIAL

4.1 The Surface Charge - Surface Potential Relationship

The relationship between the volume charge density ρ and the electric potential ψ is governed by the Poisson equation

$$\nabla(\epsilon \nabla \psi) = -4\pi\rho \tag{23}$$

subject to the boundary conditions that at the surface of the particle $\psi = \psi_0$ and in the bulk solution $\psi = \nabla\psi = 0$ where ϵ is the dielectric constant. It has been found that the dielectric constant decreases with increasing electric field strength according to the empirically determined equation (Booth, 1951)

$$\epsilon = \epsilon_0 \left[1 - B(\nabla \psi)^2\right] \tag{24}$$

where ϵ_0 is the dielectric constant at zero electric field strength and

$$1\times10^{-14} \leq B \leq 12\times10^{-14} \frac{cm^2}{volt^2}$$

Since large electric field strengths can be realized in the vicinity of a charged surface, it is necessary to determine whether the variation of the dielectric constant with field strength is significant. If an order of magnitude estimate of $\nabla\psi$ is considered as the change in ψ across the thickness of the electrical double layer, then for the one-dimensional case

$$\nabla\psi = \frac{d\psi}{dx} \sim \frac{\Delta\psi}{\Delta x} \sim \frac{\psi_0}{1/\kappa}$$

where

ψ_0 is the surface potential

x is distance

$$\kappa^2 = \frac{4\pi e^2}{\epsilon kT} \sum_i n_{i0} z_i^2$$

n_{i0} is the bulk number concentration of the i^{th} species in solution.

The fact that $1/\kappa$ is an estimate of the double layer thickness is the classical result of the Debye-Hückel theory for electrolytes.

From experimental potential versus concentration curves (see Figures 12 to 17), maximum values of the surface potential are about 150 mv and occur in the neighborhood of 10^{-4} moles/ℓ. Thus, typical values of the ionic strength and ψ_0 which will give a maximum effect are taken as 10^{-4} moles/ℓ for which $1/\kappa = 300$ Å and $\psi_0 = 150$ mv.

$$\nabla \psi \sim \frac{150\times10^{-3}\text{v}}{300\times10^{-8}\text{cm}} = 0.50\times10^{5}\ \frac{\text{volt}}{\text{cm}}$$

Then, according to Equation 24

$$\frac{\epsilon}{\epsilon_0} = 1 - 12\times10^{-14}(0.50\times10^{5})^{2} = 1 - 3.0\times10^{-4}$$

Thus, it is seen that the effect of field strength of the dielectric constant can be neglected so that the dielectric constant can be taken as being constant.

In order to determine the charge density in terms of the potential, the Boltzmann distribution is assumed to be applicable. This gives the number n_i of molecules of the i^{th} species at a position away from the surface where the potential takes on a given value as (Bikerman, 1942; Schlögl, 1954)

$$n_i = n_{i0} \exp\left[-\frac{z_i e\psi}{kT}\right] \cdot \frac{1 - \sum_j \varphi_j n_j}{1 - \sum_j \varphi_j n_{j0}} \qquad (25)$$

where φ_j is the volume of the i^{th} species. Equation 25 is a more general form of the classical Boltzmann equation in that allowance has been made for the space occupied by the molecules.

If the ratio of Equation 25 is taken for any two species, then

$$\frac{n_i}{n_j} = \frac{n_{i0}}{n_{j0}} \frac{e^{-z_i e\psi/kT}}{e^{-z_j e\psi/kT}} \tag{26}$$

Therefore, each n_j in Equation 25 can be eliminated to yield:

$$n_i = \frac{n_{i0} e^{-z_i e\psi/kT}}{1 + \sum_j \varphi_j n_{j0} e^{-z_j e\psi/kT}} \frac{1}{1 - \sum_j \varphi_j n_{j0}} \tag{27}$$

The classical Boltzmann equation assumes that the molecules are point charges with zero volume so that

$$n_i = n_{i0} \exp\left[-\frac{z_i e\psi}{kT}\right] \tag{28}$$

However, if the potential were sufficiently large, unreasonable values for the concentration near the surface would be obtained because there is no limit on how many molecules can be contained in a given volume. In order to determine whether Equation 28 is sufficient or that Equation 27 must be used, a typical calculation of the correction factors in Equation 27 will be made for a large ionic radius of 3 Å (1.1 for N_a^+, 1.81 for Cl^-), a potential of 150 mv, z = - 1, and a bulk concentration of 0.0001 mole/ℓ.

$$\varphi = \frac{4}{3}\pi (3\times10^{-8}\text{cm})^3 = 1.13\times10^{-22} \frac{\text{cm}^3}{\text{molecule}}$$

$$n_0 = 0.0001 \frac{\text{mole}}{\ell} \; 6.02\times10^{23} \frac{\text{molecules}}{\text{mole}} \; \frac{\ell}{1000\ \text{cm}^3}$$

$$= 6.02\times10^{16} \frac{\text{molecules}}{\text{cm}^3}$$

$$\varphi n_0 = 6.8\times10^{-6}$$

$$e^{-ze\psi/kT} = e^{150/25} = 403.43$$

$$\varphi n_0 e^{-ze\psi/kT} = 2.74\times10^{-3}$$

Therefore, it is seen that it is justified to use the classical form of the Boltzmann equation as given by Equation 28.

The charge density can now be determined by summing the charges of the molecules

$$\rho = \sum_i z_i e n_i \tag{29}$$

and using the Boltzmann distribution to give

$$\rho = \sum_i z_i e n_{i0} \exp\left[-\frac{z_i e\psi}{kT}\right] \tag{30}$$

Substituting Equation 30 into 23 and making use of the fact that the dielectric constant may be considered as constant, the classical Poisson-Boltzmann equation is obtained

$$\nabla^2\psi = -\frac{4\pi e}{\epsilon}\sum_i z_i n_{i0} \exp\left[-\frac{z_i e\psi}{kT}\right] \tag{31}$$

4.1.1 Planar Surfaces

Only for the planar one-dimensional case where $\nabla^2\psi = \frac{d^2\psi}{dx^2}$ can Equation 31 be integrated analytically (Parsons, 1954). Such a simplification infers that the double layer thickness is small in comparison to the radius of the particle as will be shown later. The result of a first integration is

$$\frac{d\psi}{dx} = \pm\left[\frac{8\pi kT}{\epsilon}\sum_i n_{i0}\left\{\exp\left(-\frac{z_i e\psi}{kT}\right) - 1\right\}\right]^{\frac{1}{2}} \tag{32}$$

where use has been made of the boundary condition $\psi = \frac{d\psi}{dx} = 0$ as $x \to \infty$. An expression for the surface* charge q per unit area in terms of the surface potential can now be obtained in the following way. In order to preserve electroneutrality, the surface charge must be equal to the negative of the total charge in the solution so that

$$q = -\int_0^\infty \rho dx \tag{33}$$

Eliminating ρ in Equation 33 by means of the Poisson-Boltzmann equation then gives

$$q = \frac{4\pi}{\epsilon}\int_0^\infty \frac{d^2\psi}{dx^2}\,dx = \frac{4\pi}{\epsilon}\frac{d\psi}{dx}\Bigg|_{x=0}^{x=\infty} = -\frac{4\pi}{\epsilon}\frac{d\psi}{dx}\Bigg|_{x=0} \tag{34}$$

Thus, substituting Equation 32 into 34, the surface charge in terms of surface potential ψ_0 at $x = 0$ is obtained.

$$q = \pm\left[\frac{kT\epsilon}{2\pi}\sum_i n_{i0}\left\{\exp\left(-\frac{z_i e\psi_0}{kT}\right) - 1\right\}\right]^{\frac{1}{2}} \tag{35}$$

4.1.2 Spherical Surfaces

The more difficult case of when the assumption of a planar interface is not made will now be discovered. In the case of spherical particles, the Poisson-Boltzman equation as given by Equation 31 must be written in spherical coordinates as

*What is meant by the surface from hereon is the plane which the charge resides. For example, in the case of adsorbed layers the surface would be considered as the plane of these layers and not the surface of the solid.

$$\frac{1}{r^2}\frac{d}{dr}\left(r^2\frac{d\psi}{dr}\right) = -\frac{4\pi\rho(\psi)}{\epsilon} \tag{36}$$

subject to the boundary conditions

$$\psi = \psi_0 \quad \text{at} \quad r = a$$

$$\psi = \frac{d\psi}{dr} = 0 \quad \text{as} \quad r \to \infty$$

where

r is the radial distance from the center of the particle

a is its radius.

If a different radial distance is introduced which is measured from the surface of the particle and scaled with respect to the double layer thickness according to

$$s = \kappa(r - a)$$

or

$$r = \frac{s}{\kappa} + a$$

then Equation 36 becomes

$$\frac{1}{(s/\kappa + a)^2}\frac{d}{d(s/\kappa)}\left[(s/\kappa + a)^2\frac{d\psi}{d(s/\kappa)}\right] = -\frac{4\pi\rho(\psi)}{\epsilon}$$

or

$$\frac{1}{(s + \kappa a)^2}\frac{d}{ds}\left[(s + \kappa a)^2\frac{d\psi}{ds}\right] = -\frac{4\pi\rho(\psi)}{\epsilon\kappa^2} \tag{37}$$

subject to

$$\psi = \psi_0 \quad \text{at} \quad s = 0$$

$$\psi = \frac{d\psi}{ds} = 0 \quad \text{at} \quad s \to \infty$$

Since ψ varies mainly in the double layer or between r = a and r = a + $1/\kappa$, the condition at infinity can be replaced by a finite distance. For example, numerical calculations showed that a distance of three double-layer thicknesses represented infinity very well

$$\psi = \frac{d\psi}{ds} = 0 \qquad \text{at} \qquad s = 3$$

The condition for which the solution for the planar interface approximation is valid can be easily obtained from this analysis. Equation 37 shows that as κa becomes large, it will dominate in the term "$s + \kappa a$." Since s is on the order of unity, it is seen that for values of κa much greater than one, Equation 37 reduces to that for the planar case

$$\frac{d^2\psi}{ds^2} = -\frac{4\pi\rho}{\epsilon\kappa^2}$$

In order to calculate the surface charge, one proceeds as in the planar case. The total charge Q on the particle is

$$Q = -\int_a^\infty 4\pi r^2 \rho dr = \int_a^\infty \frac{\epsilon}{4\pi} \frac{1}{r^2} \frac{d}{dr}\left(r^2 \frac{d\psi}{dr}\right) 4\pi r^2 dr$$

$$= \epsilon \int_a^\infty \frac{d}{dr}\left(r^2 \frac{d\psi}{dr}\right) dr = \epsilon r^2 \frac{d\psi}{dr}\Bigg|_a^\infty$$

$$= -\epsilon a^2 \frac{d\psi}{dr}\Bigg|_{r=a}$$

Thus, the charge q per unit surface is

$$q = Q/4\pi a^2 = -\frac{\epsilon}{4\pi} \frac{d\psi}{dr}\Bigg|_{r=a} \qquad (38)$$

For the spherical interface, an exact analytical solution is not possible. However, if the charge density ρ is expanded in series about $\psi = 0$ and only the linear term retained, a solution valid for $ze\psi_0/kT < 1$ or $\psi_0 < 25$ mv can be obtained as given by the Debye-Hückel theory (Tanford, 1961). The solution of the linearized Poisson-Boltzmann equation

$$\frac{1}{r^2}\frac{d}{dr}\left(r^2\frac{d\psi}{dr}\right) = \kappa^2\psi \tag{39}$$

subject to

$$\psi = \psi_0 \quad \text{at} \quad r = a$$

$$\psi = \frac{d\psi}{dr} = 0 \quad \text{as} \quad r \to \infty$$

yields

$$\psi = \psi_0 \frac{a}{r} \exp\left[-\kappa(r - a)\right] \tag{40}$$

$$q = \varepsilon\psi_0(1 + \kappa a)/4\pi a \tag{41}$$

For practical purposes, this solution is not very useful because the magnitude of the surface potential required for stabilization of colloidal systems greatly exceeds 25 mv by factors of 2 to 6. Therefore, the case of a spherical interface must be solved numerically by computer.

Mathematical problems of this type known as two point boundary value problems because the conditions on ψ are known at the particle surface and in the bulk solution. The problem would be relatively simple if both the potential and its derivative were known at the surface because then the non-linear differential equation could be integrated numerically like an initial value problem.

However, since the problem is to calculate the surface charge due to a given surface potential, such a procedure cannot be followed because the first derivative is proportional to the surface charge and thus not known. Fortunately on another project, the author has already developed a computer program which solves the more general multi-point boundary value problem. The basis of the numerical scheme that is employed by this program is as follows. In order to take advantage of the simplicity of solving an initial value problem, an initial guess of the first derivative or surface charge is made. This allows the differential equation to be integrated numerically from the surface to the bulk. At this point, the program checks to see whether the calculated conditions for the bulk solution are in agreement with those specified. If they are, the initial guess was correct, and the problem is solved. However, if they are not, the program calculates a first-order correction to the initial guess by means of a combination of the Newton-Raphson method and a gradient search method which insures convergence. This corrected value of the first derivative is then used to integrate the differential equation a second time. Again the bulk conditions are checked to see if they are satisfied yet. This interactive procedure continues until the bulk conditions are satisfied.

A comparison is given in Table 1 of the surface charge as calculated for a planar and spherical interface where the surface potential and ionic strength are the same. It is seen that the charge for the planar surface is smaller than that for the spherical surface but that as K_a increases the difference between them gradually decreases as expected.

Table 1

COMPARISON OF SURFACE CHARGE FOR PLANAR AND SPHERICAL SURFACES*

κa	ψ_0 (mv)	q_{planar} (coul/cm^2)	q_{sphere} (coul/cm^2)
0.660	-80	-2.660×10^{-7}	-5.163×10^{-7}
0.662	-80	-2.667×10^{-7}	-5.170×10^{-7}
0.664	-68	-2.061×10^{-7}	-4.261×10^{-7}
0.670	-40	-1.024×10^{-7}	-2.386×10^{-7}
0.682	-16	-3.827×10^{-8}	-9.376×10^{-8}
0.701	12	2.933×10^{-8}	7.101×10^{-8}
0.711	20	5.039×10^{-8}	1.196×10^{-7}
0.757	48	1.448×10^{-7}	3.055×10^{-7}
0.885	72	2.996x10-7	5.282×10^{-7}
0.990	88	4.726×10^{-7}	7.378×10^{-7}

*Data taken from the zeta potential versus concentration curve for DTAB.

a = 200 Å (see Figure 14).

4.2 The Zeta Potential

In electrophoresis experiments, the mobility of a charged particle is measured by observing the velocity at which it moves in an imposed electric field. This mobility can then be used to calculate the surface potential as discussed in detail in the literature review. Although general equations were presented, they were all based on the assumption that the viscosity in the vicinity of the particle is equal to that in the bulk solution. However, since viscosity varies with electric field strength,

this assumption may not be valid. Following Lyklema and Overbeek (1961), this problem will be investigated by modifying the Smoluchowski equation.

If the thickness of the electrical double thickness is much smaller than the radius of the particle, the liquid-solid interface can be treated as a planar surface. Then a volume element in the solution near the moving charged surface of thickness dx and unit area (see Figure 7) experiences forces due to the imposed electric field and viscosity.

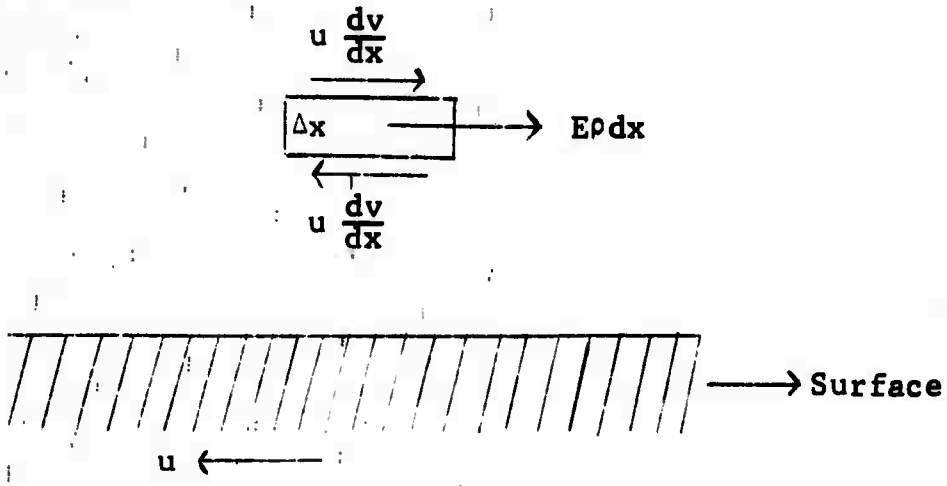

Figure 7

THE FORCES ACTING ON A VOLUME ELEMENT NEAR A CHARGED SURFACE

At steady state, the net sum of the forces must equal zero so that

$$E\rho\Delta x + \mu \left.\frac{dv}{dx}\right|_{x+\Delta x} - \mu \left.\frac{dv}{dx}\right|_{x} = 0 \qquad (42)$$

where

E is the electric field strength

μ is viscosity

v is velocity

x is distance.

Taking the limit Δx goes to zero, Equation 42 gives

$$\frac{d}{dx}\left(\mu \frac{dv}{dx}\right) = - E\rho \tag{43}$$

Eliminating ρ by means of the Poisson Equation 43 becomes

$$\frac{d}{dx}\left(\mu \frac{dv}{dx}\right) = \frac{E}{4\pi} \frac{d}{dx}\left(\epsilon \frac{d\psi}{dx}\right) \tag{44}$$

Equation 44 is integrated from the plane of shear where the velocity is equal to that of the particle u to the bulk solution where the velocity and potential gradients are zero. Due to the fact that the viscosity increases with increasing field strength, it is possible that the shear plane will not coincide with the solid surface. A first integration of Equation 44 gives

$$\frac{dv}{dx} = \frac{\epsilon E}{4\pi\mu} \frac{d\psi}{dx}$$

and a second one

$$u = \frac{E}{4\pi} \int_0^{\psi_0} \frac{\epsilon}{\mu}\, d\psi \tag{45}$$

Since mobility U is defined as

$$U = \frac{u}{E}$$

Equation 45 becomes

$$U = \frac{1}{4\pi} \int_0^{\psi_0} \frac{\epsilon}{\mu}\, d\psi \tag{46}$$

Experimental values mobilities are generally reported in terms of the zeta potential ζ which is the electric potential at the shear plane. It is assumed that the dielectric constant and

viscosity remain constant at their bulk values from the bulk to the shear plane and then from this point to the surface the viscosity becomes very large such that a viscous immobile layer is formed.

By writing Equation 46 in the form

$$U = \frac{1}{4\pi}\int_{\infty}^{0} \frac{\epsilon}{\mu}\frac{d\psi}{dx}\,dx = \frac{1}{4\pi}\int_{\infty}^{\text{shear plane}} \frac{\epsilon}{\mu}\frac{d\psi}{dx}\,dx + \int_{\text{shear plane}}^{0} \frac{\epsilon}{\mu}\frac{d\psi}{dx}\,dx \qquad (47)$$

it is seen that under these assumptions the second integral vanishes and ϵ and μ are equal to their bulk values ϵ_0 and μ_0 in the first integral so that

$$U = \frac{\epsilon_0}{4\pi\mu_0}\int_{\infty}^{\text{shear plane}} \frac{d\psi}{dx}\,dx = \frac{\epsilon_0}{4\pi\mu_0}\int_{0}^{\zeta} d\psi = \frac{\epsilon_0\zeta}{4\pi\mu_0} \qquad (48)$$

If Equations 46 and 48 are combined, then ψ_0 can be related to the measured ζ according to

$$\zeta = \frac{\mu_0}{\epsilon_0}\int_{0}^{\psi_0} \frac{\epsilon}{\mu}\,d\psi \qquad (49)$$

As noted earlier, the dependence of ϵ on field strength is given by

$$\epsilon = \epsilon_0\left[1 - B\left(\frac{d\psi}{dx}\right)^2\right] \qquad (50)$$

where $1\times10^{-14} \leq B \leq 12\times10^{-14}\ \frac{cm^2}{volt^2}$

It has also been found that the dependence of viscosity on field strength can be expressed by the empirical equation (Hunter, 1966)

$$\mu = \mu_0 \left[1 + f \left(\frac{d\psi}{dx}\right)^2\right] \tag{51}$$

where $1 \times 10^{-13} \leq f \leq 2 \times 10^{-13} \frac{cm^2}{volt^2}$

Substitution of Equations 50 and 51 into 49 yields

$$\zeta = \int_0^{\psi_0} \frac{1 - B\left(\frac{d\psi}{dx}\right)^2}{1 + f\left(\frac{d\psi}{dx}\right)^2} \, d\psi \tag{52}$$

An order of magnitude estimate of $\frac{d\psi}{dx}$ was made earlier which gave $\frac{d\psi}{dx} \sim 0.50 \times 10^5 \frac{volt}{cm}$. Inserting this result and the maximum value of f into Equation 52 gives

$$\zeta = \int_0^{\psi_0} \frac{1 - 12 \times 10^{-14} (0.50 \times 10^5)^2}{1 + 2 \times 10^{-13} (0.50 \times 10^5)^2} \, d\psi = \int_0^{\psi_0} \frac{1 - 3.0 \times 10^{-4}}{1 + 5.0 \times 10^{-4}} \, d\psi \sim \psi_0$$

This result indicates that the zeta surface potentials may be for all purposes considered equivalent. Numerical integrations of Equation 52 where $\frac{d\psi}{dx}$ was calculated from the solution of the Poisson-Boltzmann with an electric field dependent dielectric constant were made by Hunter (1966) whose results are in agreement with the above conclusion.

5. EXPLANATION OF ZETA POTENTIAL VERSUS CONCENTRATION CURVES

It is now possible to explain the shape of zeta potential versus concentration curves. From the mathematical theory presented, a pictorial description of the electrical double layer can be constructed as shown in Figure 8. A particle immersed in aqueous solution can develop a surface charge by adsorbing ions denoted as potential determining ions onto its surface. As a result of this surface charge, ions of the opposite charge will be attracted to the surface while those of the same sign will be repelled. In this way, a concentrated layer of ions oppositely charged to the surface is formed around the particle. Assuming that these ions do not adsorb onto the surface, one denotes them as counter ions. The thickness of this double layer is such that this layer contains a sufficient number of counter ions to neutralize the surface charge because the system must be electrically neutral. Thus, as the bulk concentration of counter ions increases with that of the potential determining ions remaining constant, this thickness decreases because less volume is required to contain enough counter ions to neutralize the surface charge. From an order of magnitude analysis of the Poisson equation

$$\frac{\Delta\psi}{(\Delta x)^2} \approx -\frac{4\pi}{\epsilon}\rho$$

$$\Delta\psi \approx -\frac{4\pi}{\epsilon}\rho\,(\Delta x)^2 \approx -\frac{4\pi}{\epsilon}q\,\Delta x$$

$$\psi_0 \approx \frac{4\pi}{\epsilon}q\,\Delta x$$

Therefore, the surface potential or the zeta potential follows the behavior of the double layer thickness so that they both approach zero together.

From these ideas, the concentration dependence of the zeta potential can be easily explained. With reference to Figure 1 and the $Na_2P_2O_7$ curve, when the concentration is initially

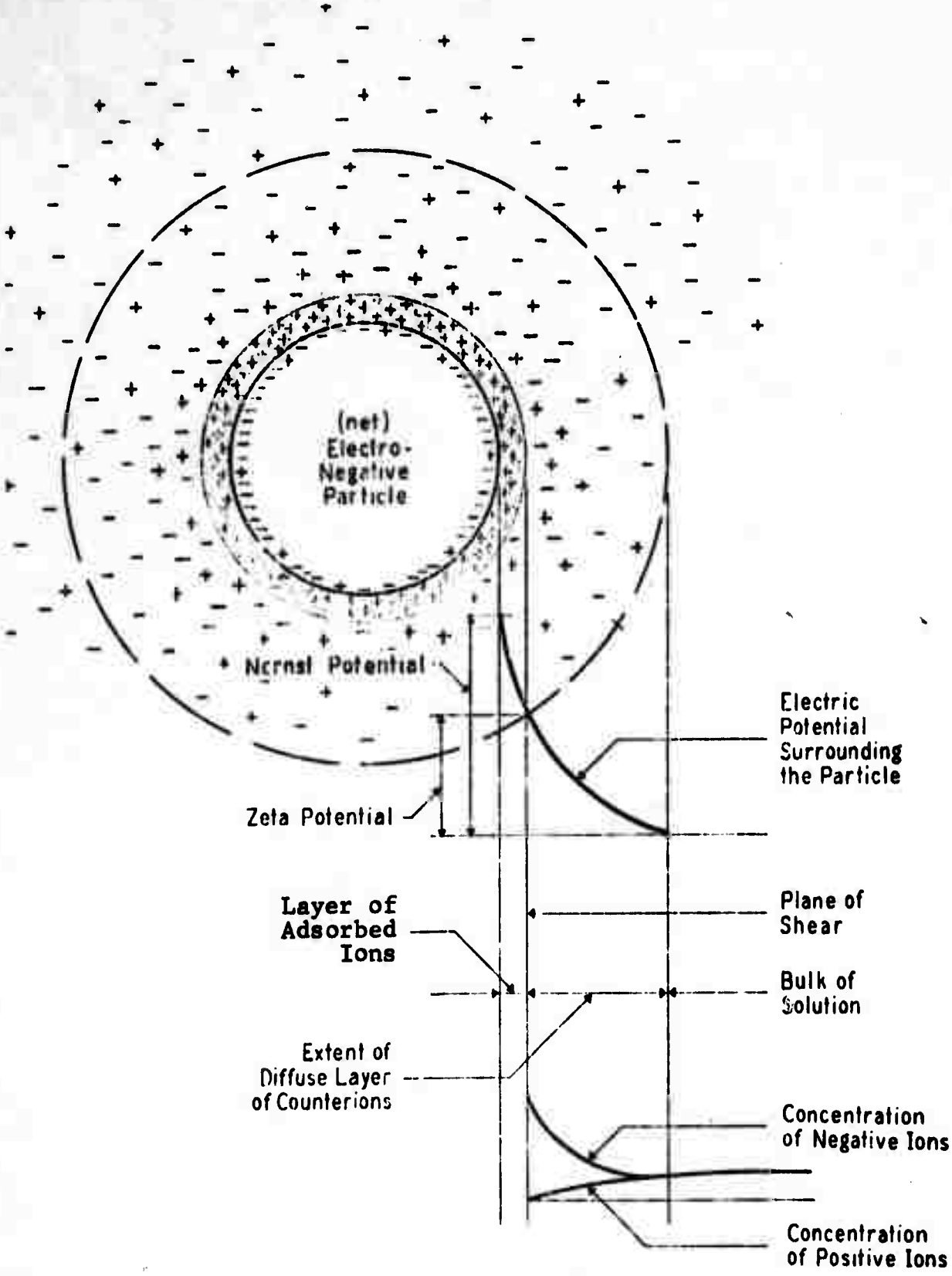

Figure 8

CONCEPT OF THE ZETA POTENTIAL
(from Riddick, 1968)

increased, the potential determining ions $P_2O_7^{-4}$ are adsorbed which decreases the magnitude of the surface charge and zeta potential while the increase in ionic strength or the concentration of counter ions Na^+ decreases it. However, at this stage, the adsorption effect is dominate so that the zeta potential decreases. However, eventually all of the surface sites become occupied so that then the ionic strength effect prevails, and the zeta potential increases to zero. In the case of $AlCl_3$, the same reasoning can be applied with the modification that positive ions are being adsorbed. As shown later, Al^{+3} ions are not adsorbed but rather its hydroxo complexes.

6. SURFACE CHARGE DUE TO CHEMICAL REACTIONS AT THE SOLID SURFACE

The surface charge on a solid can be acquired as a result of chemical reactions at the surface. Such reactions can occur because solid surfaces contain ionizable functional groups such as -OH, -COOH, $-OPO_3H_2$. Thus, the surface charge depends on the extent of ionization of these groups which in turn depends on the pH of the solution. For example, in an aqueous environment, a hydroxylated surface is formed on oxidic solids due to hydrolysis of the oxide. The surface charge then develops by means of dissociation of the surface hydroxide groups according to the reactions (Parks, 1967)

$$\text{-M-OH(S)} \rightleftharpoons \text{-M-O}^-\text{(S)} + \text{H}^+\text{(aq)} \qquad \text{(R1)}$$

$$\text{-M-OH(S)} \rightleftharpoons \text{-M}^+\text{(S)} + \text{OH}^-\text{(aq)} \qquad \text{(R2)}$$

$$\downarrow\uparrow \text{H}_2\text{O}$$

$$\text{MOH}_2^+\text{(S)}$$

where M denotes the metal and S the surface. Such a mechanism is depicted in Figure 9 for the origin of the electrical charge at the quartz surface in aqueous solutions. This reaction scheme demonstrates the amphoteric behavior of the surface in that it can act either as an acid by giving up protons (R1) or as a base by accepting protons (R2). At low pH values, the backward reaction of R1 and the forward reaction R2 will be favored so that the surface charge will be positive; on the other hand, at high pH values, the reverse will be true so that a negatively charged surface results. At some intermediate pH value denoted as the isoelectric point or zero point of charge, the surface charge will be zero.

In addition to charging due to dissociation of surface groups, charged hydroxo complexes which are formed as a result of the solubility of the solid can be adsorbed onto the solid

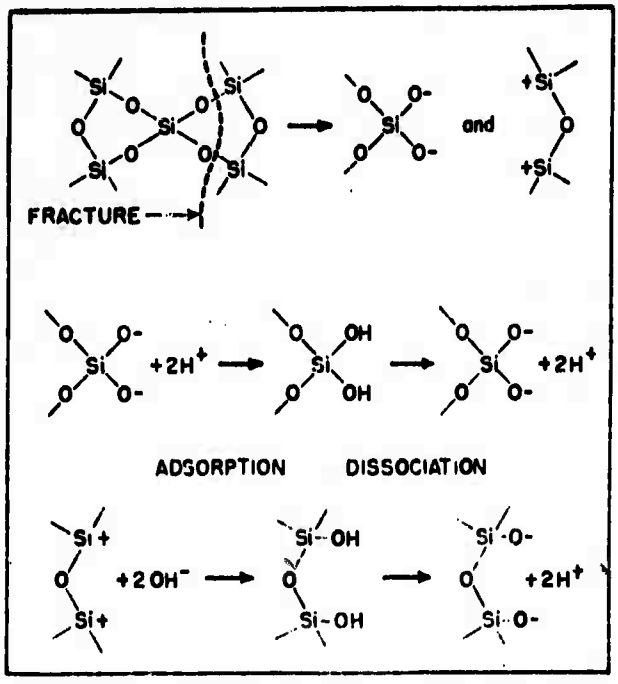

Figure 9

MECHANISM FOR THE ORIGIN OF THE ELECTRICAL CHARGE AT THE QUARTZ SURFACE IN AQUEOUS SOLUTIONS (from Gaudin and Fuerstenau, 1955)

surface. A reaction scheme for this phenomenon can be written as (Parks, 1967)

$$M_2O_3(S) + H_2O \rightleftharpoons 2M(OH)_3(aq) \rightleftharpoons 2M(OH)_n^{3-n}(aq) + 2(3-n)OH^-(aq)$$
$$\downarrow\uparrow$$
$$2M(OH)_n^{3-n}(S) \qquad \text{(R3)}$$

Possible reasons why the metal hydroxo complexes are strongly adsorbed at the surface have been given by Stumm and O'Melia (1968): (1) hydrolyzed species are larger and less hydrated than non-hydrolized species; (2) the replacement of aquo groups by

hydroxo groups in the coordination sheath of a metal ion may render a complex more hydrophobic by reducing the interaction between the central metal ion and the remaining aquo groups. This reduction in solvent-hydroxo complex interaction can then enhance the formation of covalent bonds between the metal atom and specific sites on the solid surface by reducing the energy necessary to displace water molecules from the coordination sheath. Also for polyhydroxo-polymetal species, adsorption is especially enhanced because more than one hydroxide group per molecule can become attached at the interface. In addition to metal ion hydrolysis products, most species which contain hydroxide groups in their ionic structure including both cationic and anionic hydroxo complexes adsorb at solid-liquid interfaces. For example, in the case of phosphates, ligand exchange can occur according to (Stumm and Morgan, 1970)

$$\text{-M-OH(S)} + HPO_4^{-2}(aq) \rightleftharpoons \text{-M-OPO}_3H^-(S) + OH^-(aq) \qquad \text{(R4)}$$

Hydrous metal oxides or hydroxides can also interact with cations as a coordination with electron acceptors as given by (Stumm and Morgan, 1970)

$$\text{-M-OH(S)} + A^{+z}(aq) \rightleftharpoons \text{-M-OA}^{+z}(S) + H^+(aq) \qquad \text{(R5)}$$

It is difficult to say whether these reactions are a result of coordination by covalent bond formation or electrostatic ion exchange. However, some indication can be obtained from the electronegativity by using the following empirical equation to calculate the ionic character of the bond A-B (Moore, 1964)

$$\% \text{ ionic character} = 16\,|X_A - X_B| + 3.5(X_A - X_B)^2$$

where X is the electronegativity given in Table 2. For example, in the case of the Al-O bond

$$\% \text{ ionic character} = 16\,|3.5 - 1.47| + 3.5(3.5 - 1.47)^2 = 46$$

Table 2

ELECTRONEGATIVITIES OF THE ELEMENTS
(from Moore, 1964)

H																	He
2.1																	—
Li	Be											B	C	N	O	F	Ne
0.97	1.47											2.01	2.50	3.07	3.50	4.10	—
Na	Mg											Al	Si	P	S	Cl	A
1.01	1.23											1.47	1.74	2.06	2.44	2.83	—
K	Ca	Sc	Ti	V	Cr	Mn	Fe	Co	Ni	Cu	Zn	Ga	Ge	As	Se	Br	Kr
0.91	1.04	1.20	1.32	1.45	1.56	1.60	1.64	1.70	1.75	1.75	1.66	1.82	2.02	2.20	2.48	2.74	—
Rb	Sr	Y	Zr	Nb	Mo	Tc	Ru	Rh	Pd	Ag	Cd	In	Sn	Sb	Te	I	Xe
0.89	0.99	1.11	1.22	1.23	1.30	1 36	1.42	1.45	1.35	1.42	1.46	1.49	1.72	1.82	2.01	2.21	—
Cs	Ba	*	Hf	Ta	W	Re	Os	Ir	Pt	Au	Hg	Ti	Pb	Bi	Po	At	Rn
0.86	0.97		1.23	1.33	1.40	1.46	1.52	1.55	1.44	1.42	1.44	1.44	1.55	1.67	1.76	1.90	—
Fr	Ra	**															
0.86	0.97																

*	La	Ce	Pr	Nd	Pm	Sm	Eu	Gd	Tb	Dy	Ho	Er	Tm	Yb	Lu
	1.08	1.08	1.07	1.07	1.07	1.07	1.01	1.11	1.10	1.10	1.10	1.11	1.11	1.06	1.14
**	Ac	Th	Pa	U	Np	Pu	Am	Cm	Bk	Cf	Es	Fm	Md	No	Lw
	1.00	1.11	1.14	1.22	1.22	1.22	(1.2)	(1.2)	(1.2)	(1.2)	(1.2)	(1 2)	(1.2)	(1.2)	(1.2)

Values in parentheses are estimates.

The covalent character of this bond gives some insight into why it is observed that ligands containing oxygen such as phosphates tend to adsorb onto metal oxides.

As a rule of thumb, surface coordination by covalent bonding is favored by small differences between the electronegativities of the two bonding species while large differences indicate an electrostatic interaction.

Other examples where solutes become bound to solid surfaces are (Stumm and Morgan, 1970)

$$FeOOH(S) + H^+(aq) \rightleftharpoons Fe(OH)_2^+(S)$$

$$FeOOH(S) + OH^-(aq) + H_2O \rightleftharpoons Fe(OH)_4^-(S)$$

$$FePO_4(S) + H_2PO_4^-(aq) \rightleftharpoons Fe(HPO_4)_2^-(S)$$

$$SiO_2(S) + OH^- \rightleftharpoons SiO_2(OH)^-(S)$$

$$AgBr(S) + Br^- \rightleftharpoons AgBr_2^-(S)$$

$$Cu(S) + 2H_2S \rightleftharpoons Cu(SH)_2^{-2}(S) + 2H^+(aq)$$

$$S(S) + S^{-2}(aq) \rightleftharpoons S_3^{-2}(S)$$

$$R(COOH)_n(S) + mCa^{+2} \rightleftharpoons R\text{-}\left[(COO)_nCa_m\right]^{-n+2m}(S) + nH^+(aq)$$

$$MnO_2 \cdot H_2O(S) + Zn^{+2} \rightleftharpoons MnOOHOZn^+(S) + H^+(aq)$$

It is of interest to note that when adsorption results due to surface chemical reactions, it can occur against electrostatic repulsion forces because the energy released due to the chemical reaction can outweigh the electrostatic work involved in bringing the adsorbant from the bulk to the surface.

The composition and properties or simply the reactivity of the solid plays an important role in determining the surface reactions which occur and to what extent. For example, Table 3 shows that the isoelectric point for aluminum oxide can vary from pH 5 to pH 9.25 as a result of different modifications of the material and different active forms of the same modification. A summary of the transformations of the various crystalline modification of aluminum oxide and hydroxide is shown in Figure 10.

Table 3

ISOELECTRIC POINTS OF ALUMINUM OXIDE
(from Parks, 1965)

Material	zpc (pH)
α-Al_2O_3	5.0, 6.6, 9.2
ν-Al_2O_3	8.0
α-AlOOH	7.7, 9.1
α-$Al(OH)_3$	5.0
ν-$Al(OH)_3$	9.25

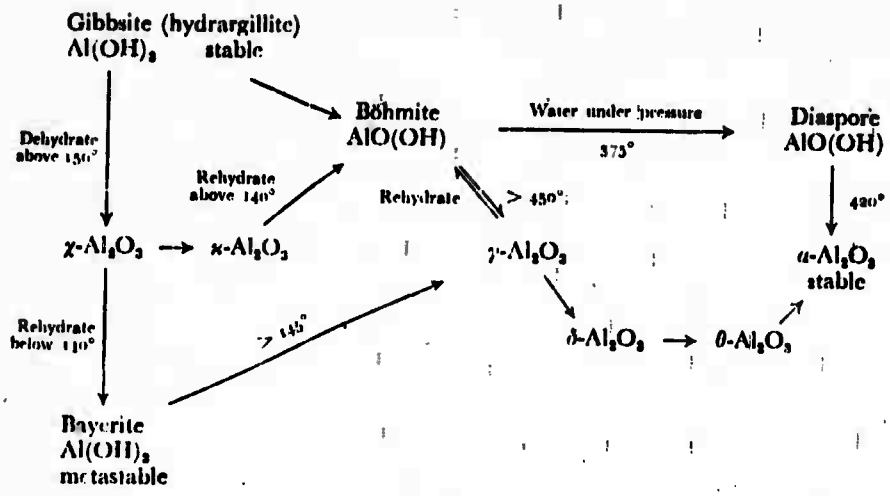

Figure 10

SUMMARY OF THE TRANSFORMATIONS OF THE VARIOUS CRYSTALLINE MODIFICATIONS OF THE ALUMINUM OXIDES AND HYDROXIDES (from Remy, 1956)

Active forms of a material are very fine crystalline precipitates with a disordered lattice and are generally formed incipiently from strongly oversaturated solutions. Active forms convert into more stable or inactive forms although such transformations may proceed slowly. Inactive or aged forms have ordered crystals and are thus less soluble than active forms. Hydroxides and sulfides are examples of materials which occur in amorphous and several crystalline modifications. In the case of iron hydroxide, the amorphous active form can age to the inactive form and to more stable modifications according to the scheme.

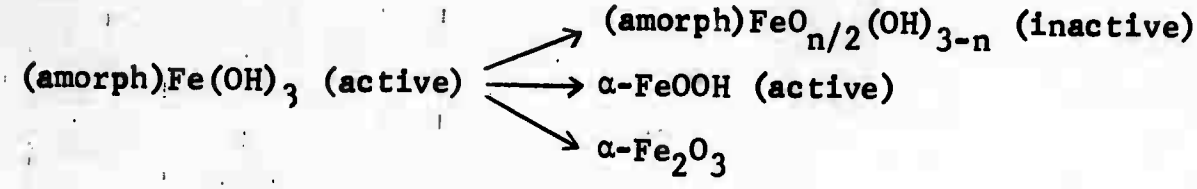

6.1 Surface Charges Due to Adsorption of Complex Ions Derived from Electrolytes

It has been shown in many studies that multivalent metals ions react with water or hydrolyze to produce a variety of complex ions. For the case of trivalent metal ions such Al^{+3} and Fe^{+3}, the successive acid-base reactions are (Sullivan and Singley, 1968)

$$M(H_2O)_6^{+3} \rightleftharpoons M(H_2O)_5OH^{+2} + H^+$$
$$\rightleftharpoons M(H_2O)_4(OH)_2^+ + 2H^+ \rightleftharpoons M(OH)_3(H_2O)_3 + 3H^+$$
$$\rightleftharpoons M(OH)_4(H_2O)_2^- + 4H^+ \rightleftharpoons M(OH)_5H_2O^{-2} + 5H^+$$
$$\rightleftharpoons M(OH)_6^{-3} + 6H^+ \qquad \text{(R6)}$$

For bivalent ions, such as Zn^{+2} and Cu^{+2}, a similar reaction scheme is followed except that only four water molecules instead of six can be coordinated with the metal ion.

In addition to these hydroxo complexes, polynuclear hydroxo complexes are formed through polymerization of the hydroxo complexes by condensation reaction such as

$$2M(H_2O)_5OH^{+2} \rightleftharpoons \left[(H_2O)_4M\begin{matrix}OH\\ \diagup\ \diagdown\\ OH\end{matrix}M(H_2O)_4\right]^{+4} + 2H_2O \qquad \text{(R7)}$$

This dimer can then hydrolyze to provide hydroxo groups so that another condensation reaction can occur. For aluminum, the

accepted general form of such polynuclear species is $Al_n(OH)_{2.5x}^{+0.5x}$ (Brossett, 1954). The main complexes with this formula which have been suggested by various investigators are $Al_6(OH)_{15}^{+3}$ (Brossett, 1954) and $Al_8(OH)_{20}^{+4}$ (Matijevic, 1961) and others such as $Al_7(OH)_{17}^{+3}$ (Hsu, 1965) and $Al_{13}(OH)_{34}^{+5}$ (Rausch, 1964). These polynuclear complexes have been proposed to fit into the hydrolysis reactions as intermediates between $Al(H_2O)_4(OH)_2^+$ and $Al(OH)_3(H_2O)_3$ as shown in Figure 11 (Stumm and Morgan, 1962). Equilibrium constants for hydrolysis and complex formation for aluminum and iron are given in Table 4.

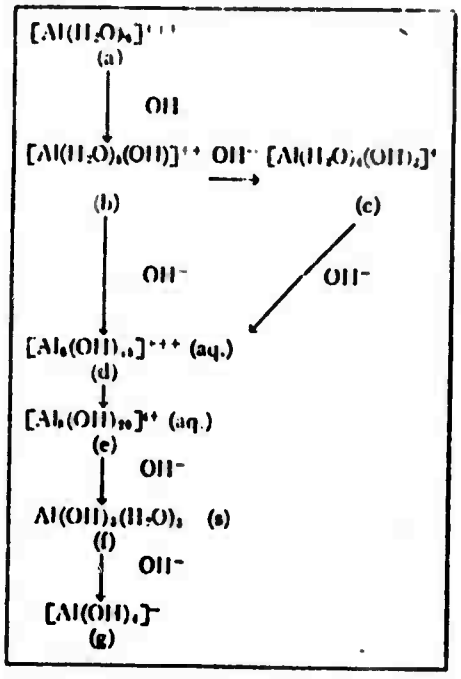

Figure 11

STEPWISE CONVERSION OF THE TRI-POSITIVE ALUMINUM ION TO THE NEGATIVE ALUMINATE ION (from Stumm and Morgan, 1962)

Table 4

HYDROLYSIS AND COMPLEX FORMATION EQUILIBRIA
OF IRON AND ALUMINUM
(from Stumm and Morgan, 1970)

No.	Equilibrium	Log of Equilibrium Constant* (25°C)
1	$[Fe(H_2O)_6]^{+++} + H_2O = [Fe(H_2O)_5OH]^{++} + H_3O^+$	− 2.17
2	$[FeOH]^{++} + H_2O = [Fe(OH)_2]^+ + H^+$	− 4.7
3	$2[FeOH]^{++} = [Fe_2(OH)_2]^{++++}$	1.46
4	$Fe^{+++} + 3H_2O = Fe(OH)_3\ (s) + 3H^+$	− 6
5	$Fe(OH)_3\ (s) + H_2O = [Fe(OH)_4]^- + H^+$	−18.5
6	$Al^{+++} + H_2O = [AlOH]^{++} + H^+$	− 5.01
7	$2Al^{+++} + 2H_2O = [Al_2(OH)_2]^{++++} + 2H^+$	− 6.27
8	$Al^{+++} + 3H_2O = Al(OH)_3\ (s) + 3H^+$	− 9.1
9	$Al(OH)_3\ (s) + H_2O = [Al(OH)_4]^- + H^+$	−12.56
10	$8Al^{+++} + 20H_2O = [Al_8(OH)_{20}]^{++++} + 20\ H^+$	
11	$6Al^{+++} + 15H_2O = [Al_6(OH)_{15}]^{+++} + 15H^+$	163
12	$Fe^{+++} + SO_4^{--} = FeSO_4^+$	2.23
13	$Fe^{+++} + HPO_4^{---} = [FeHPO_4]^+$	8.4
14	$Fe^{+++} + PO_4^{---} = FePO_4\ (s)$	21.9
15	$Al^{+++} + PO_4^{---} = AlPO_4\ (s)$	22
16	$Fe^{+++} + P_2O_7^{----} = [FeP_2O_7]^-$	
17	$Al^{+++} + P_2O_7^{----} = [AlP_2O_7]^-$	
18	$Fe^{+++} + F^- = [FeF]^{++}$	5.17
19	$Al^{+++} + F^- = [AlF]^{++}$	6.13
20	$Fe^{+++} + Acetate^- = [Fe\ Acetate]^{++}$	
21	$Al^{+++} + 3\ Acetate^- = [Al\ (Acetate)_3]$	
22	$Fe^{+++} + 3\ Oxalate^{--} = [Fe(Oxalate)_3]^{---}$	21.9
23	$Al^{+++} + 3\ Oxalate^{--} = [Al(Oxalate)_3]^{---}$	16.1
24	$Fe^{+++} + Phenolate^- = [Fe\ Phenolate]^{++}$	8.2
25	$Fe^{+++} + Citrate^{---} = [Fe\ Citrate]^+$	25
26	$Fe^{+++} + Salicylate^{--} = [Fe\ Salicylate]^+$	15.82
27	$Al^{+++} + Salicylate^{--} = [Al\ Salicylate]^+$	14

Compounds that are commonly used to supply aluminum and ferric ions in solution for the purpose of stabilization and destabilization of colloids by hydrolyzed metal ions are $FeCl_3$, $Fe(ClO_4)_3$, $Al_2(SO_4)_3$, and alums such as $R_2^{I}SO_4R_2^{III}(SO_4)_3(H_2O)_{24}$ or $R^{I}R^{III}(SO_4)_2(H_2O)_{12}$ where R^{I} denotes an univalent metal such as sodium or potassium and R^{III} is either Al^{+3} or Fe^{+3}.

In order to demonstrate how these ideas can be put into a quantitative form, let us consider the hydrolysis of a trivalent

metal without polynuclear complex formation which can be represented as

$$M(H_2O)_{7-i}(OH)_{i-1}^{4-i} \underset{}{\overset{k_i}{\rightleftharpoons}} M(H_2O)_{6-i}(OH)_i^{3-i} + H^+ \quad i=1,2,.....,6$$

species i — species i + 1 (R8)

The equilibrium relationships are then given by

$$K_i = \frac{c_{i+1}[H^+]}{c_i} \qquad i=1,2,.....,6 \tag{53}$$

where c denotes concentration.

If it is assumed that the amount of metal ions adsorbed onto the solid is small in comparison to the amount initially supplied to the solution through an electrolyte, a mass balance on M neglecting the adsorbed species yields

$$\sum_{j=1}^{7} c_j = c_0 \tag{54}$$

where c_0 is the initial or total concentration of M.

Since, from Equation 53

$$c_{i+1} = \frac{K_i}{[H^+]} c_i$$

one may proceed by induction to show that

$$c_2 = \frac{K_1}{[H^+]} c_1$$

$$c_3 = \frac{K_2}{[H^+]} c_2 = \frac{K_1 K_2}{[H^+]^2} c_1$$

$$\vdots$$

$$c_{k+1} = \frac{\prod_{j=0}^{k} K_j}{[H^+]^k} c_1 \qquad (55)$$

$$\vdots$$

$$c_7 = \frac{K_1 K_2 K_3 K_4 K_5 K_6}{[H^+]^6} c_1$$

where $K_0 = 1$ and π denotes the product sign.

Substituting Equation 55 into 54

$$\sum_{i=0}^{6} \frac{\prod_{j=0}^{i} K_j}{[H^+]^i} c_1 = c_0$$

so that

$$c_1 = \frac{c_0}{\sum_{i=0}^{6} \frac{\prod_{j=0}^{i} K_j}{\left[H^+\right]^i}} \tag{56}$$

Thus, the concentration of the $k+1^{th}$ species is obtained by substituting Equation 56 into 55

$$c_{k+1} = \frac{c_0 \prod_{j=0}^{k} K_j / \left[H^+\right]^k}{\sum_{i=0}^{6} \prod_{j=0}^{i} K_j / \left[H^+\right]^i} \qquad k=0,1,.....,6 \tag{57}$$

In order to calculate the surface charge due to adsorption of the hydroxo complexes, Equation 15 derived earlier for surface charging due to multi-component single layer adsorption is used. It has been suggested that the specific adsorption energies for all the complexes are approximately equal (Parks and de Bruyn, 1962).

Complex formation is not restricted to hydroxides but other groups such as phosphates can also undergo complex formation. When a phosphate such as KH_2PO_4 is put into solution, the following equilibria reactions occur

$$\underset{\text{species 1}}{H_3PO_4} \overset{k_1}{\rightleftharpoons} \underset{\text{species 2}}{H_2PO_4^-} + H^+ \overset{k_2}{\rightleftharpoons} \underset{\text{species 3}}{HPO_4^{-2}} + 2H^+$$

$$\overset{k_3}{\rightleftharpoons} \underset{\text{species 4}}{PO_4^{-3}} + 3H^+ \tag{R9}$$

The concentrations of the various species are given by Equation 57 where k = 0,1,2,3 and the summation in the denominator ranges from 0 to 3.

Equilibrium constants for the hydrolysis reactions of various phosphates are given in Table 5.

Table 5

ACIDITY AND HYDROLYSIS OF PHOSPHATES AND METAL IONS
(from Stumm and Morgan, 1970)

No.	Equilibrium	Log Equilibrium Constant, 25°C
8	$H_3PO_4 = H_2PO_4^- + H^+$	−2.2
9	$H_2PO_4^- = HPO_4^{2-} + H^+$	−7.0
10	$HPO_4^{2-} = PO_4^{3-} + H^+$	−12.0
11	$H_3P_2O_7^- = H_2P_2O_7^{2-} + H^+$	−2.4
12	$H_2P_2O_7^{2-} = HP_2O_7^{3-} + H^+$	−6.6
13	$HP_2O_7^{3-} = P_2O_7^{4-} + H^+$	−9.3
14	$H_3P_3O_{10}^{2-} = H_2P_3O_{10}^{3-} + H^+$	−2.3
15	$H_2P_3O_{10}^{3-} = HP_3O_{10}^{4-} + H^+$	−6.5
16	$HP_3O_{10}^{4-} = P_3O_{10}^{5-} + H^+$	−9.2
17	$HP_3O_9^{2-} = P_3O_9^{3-} + H^+$	−2.1

These phosphates can then adsorb onto hydrous metal oxides or hydroxides by ligand exchange according to (Stumm and Morgan, 1970)

$$-M\text{-}OH(S) + HPO_4^{-2}(aq) \rightleftharpoons -M\text{-}OPO_3H^-(S) + OH^-(aq) \qquad (R10)$$

Although OH^- has a greater affinity for metal ions such as Fe^{+3} than the phosphates do, the adsorption of the phosphates is favored by reduction in pH. However, this reduction is limited by the hydrolysis equilibria of the phosphates because as pH is decreased the fraction of the ionized phosphates will decrease. In order to calculate the surface charge due to phosphate adsorption, Equation 15 for multi-component adsorption may again be used.

6.2 Surface Charge Due to Adsorption of Complex Ions Derived from the Solid

Due to the solubility of the solid, metal ions are introduced into the solution and can then subsequently hydrolyze to form hydroxo complexes. The amount of metal ions obtained from the solid can be described by

$$\frac{1}{2}M_2O_3^{(S)} + \frac{3}{2}H_2O \rightleftharpoons M^{+3} + 3OH^- \qquad \text{(R11)}$$

or

$$M(OH)_3^{(S)} \rightleftharpoons M^{+3} + 3OH^- \qquad \text{(R12)}$$

with the solubility product given by

$$K_{sp} = \left[M^{+3}\right]\left[OH^-\right]^3 \qquad (58)$$

It is also possible that hydroxo complexes will be formed according to

$$M(OH)_3 \rightleftharpoons M(OH)_n^{3-n} + (3 - n)OH^-$$

However, the solubility products of such reactions are much smaller than for the former so that these reactions will be neglected.

In order to calculate the concentrations of the complexes in solution, Equation 58 is solved in conjunction with Equation 53. Therefore, substituting Equation 58 for c_1 into 55, the concentrations of the complexes are

$$c_{k+1} = \frac{K_{sp}\prod_{j=1}^{k} K_j}{\left[OH^-\right]^3\left[H^+\right]^k} \qquad k=0,1,\ldots,6 \qquad (59)$$

The surface charge is then determined as before by the Equation 15 for surface charging due to multi-component single layer adsorption.

6.3 Surface Charge Due to Dissociation of Surface Groups

Oxides of tri-valent metals such as aluminum and iron have the corundum lattice in which the oxygen ions are arranged in hexagonal packing with each metal ions coordinated by six oxygen ions and each oxygen ion by four metal ions. As discussed earlier, at a freshly fractured surface, the coordination of some ions will be incomplete so that hydroxyl ions in solution will react with metal ions and protons with the oxygen ions. In this manner, hydroxyl groups are formed on the solid surface and can ionize as bases or acids to produce a surface charge. The degree to which the surface is disturbed determines how hydroxylated the surface is. Those parts of the surface severely distorted are hydroxylated completely to $M(OH)_3$ while less distorted areas are only partly hydroxylated to MO·OH (O'Connor et al., 1956).

The extent to which the surface hydroxyl groups ionize as acids or bases depends on how polarized they are by the coordinating metal ions. Because MO·OH has two bonds and $M(OH)_3$ three, it is expected that the hydroxyl groups are more polarized in MO·OH than in $M(OH)_3$ suggesting that the character of MO·OH is acidic acid and $M(OH)_3$ basic (O'Connor et al., 1956). On this basis, MO·OH can dissociate according to

$$MO^+(S) + 2H_2O \overset{K_{p1}}{\rightleftharpoons} MO\cdot OH(S) + H_3O^+(aq)$$

$$MO\cdot OH(S) + H_2O \overset{K_{p2}}{\rightleftharpoons} MO_2^-(S) + H_3O^+(aq) \qquad \text{(R13)}$$

and $M(OH)_3$ according to

$$M^{+3}(S) + 2H_2O \overset{K_{c1}}{\rightleftharpoons} M(OH)^{+2}(S) + H_3O^+(aq)$$

$$M(OH)^{+2}(S) + 2H_2O \overset{K_{c2}}{\rightleftharpoons} M(OH)_2^+(S) + H_3O^+(aq)$$

$$M(OH)_2^+(S) + 2H_2O \overset{K_{c3}}{\rightleftharpoons} M(OH)_3(S) + H_3O^+(aq) \qquad \text{(R14)}$$

$$M(OH)_3(S) \overset{K_{c4}}{\rightleftharpoons} MO_2^-(S) + H_3O(aq)$$

where the subscripts p and c denote the partially and completely hydrated oxide, respectively.

The negative group MO_2^- was chosen instead of $M(OH)_4^-$ because it is unlikely that a coordination number of seven would be realized.

From this mechanism, it is seen that at low pH values the surface charge will be positive because the backward reactions are favored while at high pH it will be negative because the forward ones are favored.

Due to electrostatic interaction, removal of a proton becomes progressively more difficult as the charge on the surface group decreases from a high positive value to a negative. This suggests the following sequence for the magnitude of the equilibrium constants

$$K_{p1} > K_{p2}$$

$$K_{c1} > K_{c2} > K_{c3} > K_{c4}$$

Also, at the isoelectric point assuming only the presence of uni-valent species

$$K_{p1} = \frac{\left[MO\cdot OH\right]\left[H^+\right]_{zpc,p}}{\left[MO^+\right]}$$

$$K_{p2} = \frac{\left[MO_2^-\right]\left[H^+\right]_{zpc,p}}{\left[MO\cdot OH\right]}$$

so that

$$\left[H^+\right]^2_{zpc,p} = K_{p1}K_{p2}\frac{\left[MO^+\right]}{\left[MO_2^-\right]} = K_{p1}K_{p2} \qquad (60)$$

since for zero surface charge $\left[MO^+\right] = \left[MO_2^-\right]$.

Similarly,

$$\left[H^+\right]^2_{zpc,c} = K_{c3}K_{c4} \qquad (61)$$

Thus, the ratio of the isoelectric points is

$$\frac{\left[H^+\right]_{zpc,p}}{\left[H^+\right]_{zpc,c}} = \sqrt{\frac{K_{p1}}{K_{c3}}\,\frac{K_{p2}}{K_{c4}}} \qquad (62)$$

As indicated above, hydroxyl groups are more polarized in MO·OH than in $M(OH)_3$ which means that

$$K_{p1} > K_{c3}$$

$$K_{p2} > K_{c4}$$

Therefore,

$$\left[H^+\right]_{zpc,p} > \left[H^+\right]_{zpc,c} \qquad (63)$$

On the basis of these facts, one concludes that metal oxides which are extensively hydrated to form a surface layer of predominately $M(OH)_3$ have their isoelectric points in basic solution

and are positively charged in neutral solution; on the other hand, metal oxides which are partially hydrated have their isoelectric points in acid solution and are negatively charged in neutral solution. For intermediate degrees of hydration, the surface consists of a mixture of $M(OH)_3$ and $MO \cdot OH$ which accounts for the wide range of isoelectric points of oxides and its dependence on the treatment of the material such as grinding, heating, ignition, and aging under water. These conclusions are in agreement with experimental observations for alumina or Al_2O_3 (O'Connor et al., 1956; Parks, 1965; Robinson et al., 1964).

The magnitude of the surface charge can be expressed quantitatively by proceeding as in the previous analyses. By noting the similarity of the reaction mechanisms for dissociation of surface groups and hydroxo complex formation, the surface charge due to dissociation can be easily deduced. The total charge due to the complexes is

$$q = \sum_{i=1}^{7} z_i e c_i$$

where c_i is given by Equation 57. Multiplying both numerator and denominator of this expression by $\frac{[H^+]^3}{K_1 K_2 K_3}$ one obtains

$$q = c_0 e \left\{ \frac{z_1 \left[H^+\right]^3}{K_1 K_2 K_3} + \frac{z_2 \left[H^+\right]^2}{K_2 K_3} + \frac{z_3 \left[H^+\right]}{K_3} + \cancel{z_4}^{\,0} + \frac{z_5 K_4}{\left[H^+\right]} + \frac{z_6 K_4 K_5}{\left[H^+\right]^2} + \frac{z_7 K_4 K_5 K_6}{\left[H^+\right]^3} \right\} \Bigg/ \left\{ \frac{\left[H^+\right]^3}{K_1 K_2 K_3} + \frac{\left[H^+\right]^2}{K_2 K_3} + \frac{\left[H^+\right]}{K_3} + 1 + \frac{K_4}{\left[H^+\right]} + \frac{K_4 K_5}{\left[H^+\right]^2} + \frac{K_4 K_5 K_6}{\left[H^+\right]^3} \right\} \qquad (64)$$

In order to eliminate the extra reactions in hydroxo complex formation not present in surface dissociation, one sets

$$K_1 = K_2 = \infty$$

$$K_3 = K_{p1}$$

$$K_4 = K_{p2}$$

$$K_5 = K_6 = 0$$

$$c_0 = N_p$$

for the surface charge contribution due to dissociation of MO·OH, and

$$K_1 = K_{c1}$$

$$K_2 = K_{c2}$$

$$K_3 = K_{c3}$$

$$K_4 = K_{c4}$$

$$K_5 = 0$$

$$K_6 = 0$$

$$c_0 = N_c$$

for the surface contribution due to dissociation of $M(OH)_3$. N_p and N_c denote the total number of sites which are partially and completely hydrated to provide the available sites for the dissociation of $MO{\cdot}OH$ and $M(OH)_3$, respectively. Thus, the surface charge due to dissociation is given by

$$q = N_p e \left\{ \frac{[H^+]}{K_{p1}} - \frac{K_{p2}}{[H^+]} \right\} \Bigg/ \left\{ \frac{[H^+]}{K_{p1}} + 1 + \frac{K_{p2}}{[H^+]} \right\}$$

$$+ N_c e \left\{ \frac{3[H^+]^3}{K_{c1}K_{c2}K_{c3}} + \frac{2[H^+]^2}{K_{c2}K_{c3}} + \frac{[H^+]}{K_{c3}} - \frac{K_4}{[H^+]} \right\} \Bigg/$$

$$\left\{ \frac{[H^+]^3}{K_{c1}K_{c2}K_{c3}} + \frac{[H^+]^2}{K_{c2}K_{c3}} + \frac{[H^+]}{K_{c3}} + 1 + \frac{K_4}{[H^+]} \right\} \qquad (65)$$

Due to the fact that these dissociation reactions are occuring on a charged surface, the values of the equilibrium constants will be a function of the surface charge because it becomes progressively more difficult to remove a proton from the surface as the surface charge decreases from a positive value to a negative one.

This effect on the equilibrium constants can be determined if it is recalled from classical thermodynamics that the equilibrium constant and free energy change ΔG per molecule of a reaction are related by

$$\Delta G = - kT \ln K \qquad (66)$$

By determining the change in ΔG as a result of reaction on a charged surface, the corresponding change in K is obtained.

Although the surface charge consists of discrete charges, it is mathematically convenient to treat this charge as being uniformly smeared over the surface (Tanford, 1961). This assumption means that the free energy of a surface molecule is being

considered equal to the average free energy of the surface per molecule. Thus, when a proton of charge ze is removed from a surface of charge q, the contribution to the change dG in the free energy G of the surface due to electrical interaction is

$$dG_{el} = -\frac{\partial G}{\partial q} ze$$

Since the free energy is given by the work to charge the surface,

$$G_{el} = \int_0^q \psi(q')dq'$$

Differentiation under the integral sign yields

$$\frac{\partial G_{el}}{\partial q} = \psi_0$$

so that

$$dG_{el} = -ze\psi_0$$

Therefore, if ΔG° is the free energy change per molecule of the reaction occuring on an uncharged surface, then ΔG for a charged surface of electrical potential ψ_0 is given by

$$\Delta G = \Delta G^\circ - ze\psi_0 \qquad (67)$$

Combining Equation 66 and 67, the equilibrium constant can be written as

$$K = \exp\left(\frac{-\Delta G^\circ + ze\psi_0}{kT}\right) \qquad (68)$$

where the presence of the electrical surface potential reflects the surface charge dependence. The relationship between the surface charge and surface potential has been discussed in Section 4.1.

If ΔG° is replaced by its corresponding equilibrium constant for reaction on an uncharged surface, then

$$K = K_0 \exp\left(\frac{ze\psi_0}{kT}\right) \tag{69}$$

where

$$K_0 = \exp\left(-\frac{\Delta G^\circ}{kT}\right)$$

7. EXPLANATION OF THE SURFACE CHARGE VERSUS CONCENTRATION CURVE

One is finally in a position to explain the dependence of the adsorption density of potential determining ions and the resulting surface charge on these ions and the ionic strength.

When the surface charge is a result of adsorption from solution, it is seen from the multi-component adsorption isotherm given by Equation 15 that the charge varies with

$$b_i = \exp\left[-\frac{\Delta G_i^0}{kT}\right] = \exp\left[-\frac{\psi_i + z_i e\psi_0}{kT}\right]$$

When the surface is positively charged, positive ions are being adsorbed so that z_i and ψ_0 are positive and thus also $z_i e\psi_0$. Since the specific adsorption energy ψ_i is negative, a decrease in ψ_0 makes ΔG_i^0 more negative and thus increases b_i and accordingly also the surface charge. Since an increase in ionic strength decreases the double layer thickness and thus also the surface potential, the above reasoning shows that the surface charge increases with increasing ionic strength as found experimentally. Similarly, for a negatively charge surface, the term $z_i e\psi_0$ is again positive which shows that the surface charge becomes more negative with increasing ionic strength. Also, since $\psi_0 = 0$ at the isoelectric point, it is seen that this point is independent of ionic strength in agreement with experimental observation.

In the case when surface dissociation determines the surface charge, one notes that the equilibrium constant is a function of the surface potential according to

$$K = K_0 \exp\left(\frac{ze\psi_0}{kT}\right)$$

where $z = 1$ for H^+.

For a positively charged surface, an increase in ionic strength makes ψ_0 less positive which in turn decreases K. This

means that the backward acid-base reactions occuring on the surface are favored so that the charge becomes more positive. Similarly, for a negatively charged surface increasing ionic strength makes ψ_0 less negative which in turn increases K. This means that the forward reactions are favored so that the charge becomes more negative. Also, at the zero point charge, the surface potential is zero so that the equilibrium constants and thus the isoelectric point are independent of ionic strength. Again, these conclusions are in agreement with experimental observations.

8. VERIFICATION OF THEORETICAL MODELS

8.1 Comparison of Adsorption Theory with Experimental Data

The theory presented for the adsorption of ions from solution onto solid surfaces will now be compared with experimental data. The studies of Ottewill and Rastogi (1960) will be used for this purpose. They measured the zeta potential of silver iodide solutions at pI 4 in the presence of several cationic polyelectrolytes. The radius of the particles was 200 Å.

In the absence of polyelectrolytes, the particles had a value of $K_a = 0.66$ and a zeta potential of -80 mv due to excess iodide ions in their surfaces. It is assumed that the contribution to the surface charge due to this excess of surface iodide ions is not significantly affected by the addition of a polyelectrolyte. Thus, the system was treated as the adsorption of one species onto particles with an initial given charge.

The ionic strength was calculated from the concentrations of AgI and the polyelectrolyte in solution. The surface charge and zeta potential were related through Equation 35 for a planar surface. Although the value of K_a does not warrant the use of Equation 35, it was nevertheless used because it became too time-consuming to utilize the computer program for a spherical surface. This was a result of the large number of calculations required for use as input to the regression analysis. The adsorption isotherm used for predicting the surface charge was that given by the multi-layer adsorption Equation 22 for a single component. This isotherm was used because it is known that polyelectrolyte molecules can adsorb onto themselves to form a second adsorption layer. Also, the total adsorption energy term was assumed to be just the specific adsorption energy with the exclusion of the surface potential term because the latter is small in comparison with the former term. Under these assumptions, the model simplifies to one similar to that proposed in the papers of Ottewill

which is limited to $\zeta < 25$ mv and one component system.

The values of the parameters N_0, ΔG_1^0, and ΔG_{11}^0 were obtained by regression analysis subject to the constraint that the ζ versus c curves passed through the measured isoelectric point. A computer program was developed for this purpose. The values obtained for the available number of surface sites and the adsorption energies were on the order of 10^{13} sites/cm^2 and 10 Kcal/mole which is in agreement with commonly accepted values. Also, the adsorption energies for the first layer were always greater in absolute magnitude than those for the second which is what one would expect.

The ζ versus c curves as predicted by the theory is compared with experimental data in Figures 12 to 17 for various polyelectrolytes. It is seen that there is in general good agreement between theory and experiment. The discrepancies which do occur in some of the figures are around 10^{-4} M where ζ is overestimated. This is a result of treating the surface as planar and to the lesser neglecting the surface potential contribution to the adsorption energy and can be shown qualitatively by using the Debye-Hückel approximation (Equation 41). The potential due to a surface charge for a spherical surface is

$$\psi_{OS} = \frac{4\pi aq}{\epsilon(1 + \kappa a)}$$

and for a planar one

$$\psi_{OP} = \frac{4\pi q}{\epsilon\kappa}$$

The ratio of these two equations gives

$$\psi_{OS} = \frac{\kappa a}{1 + \kappa a} \psi_{OP} \qquad (70)$$

Since the AgI concentration was maintained at 10^{-4} M which corresponds to $\kappa a = 0.66$, it is seen that κa does not vary significantly until the polyelectrolyte concentration approaches 10^{-5} M. In this concentration range, the κa term acts like a

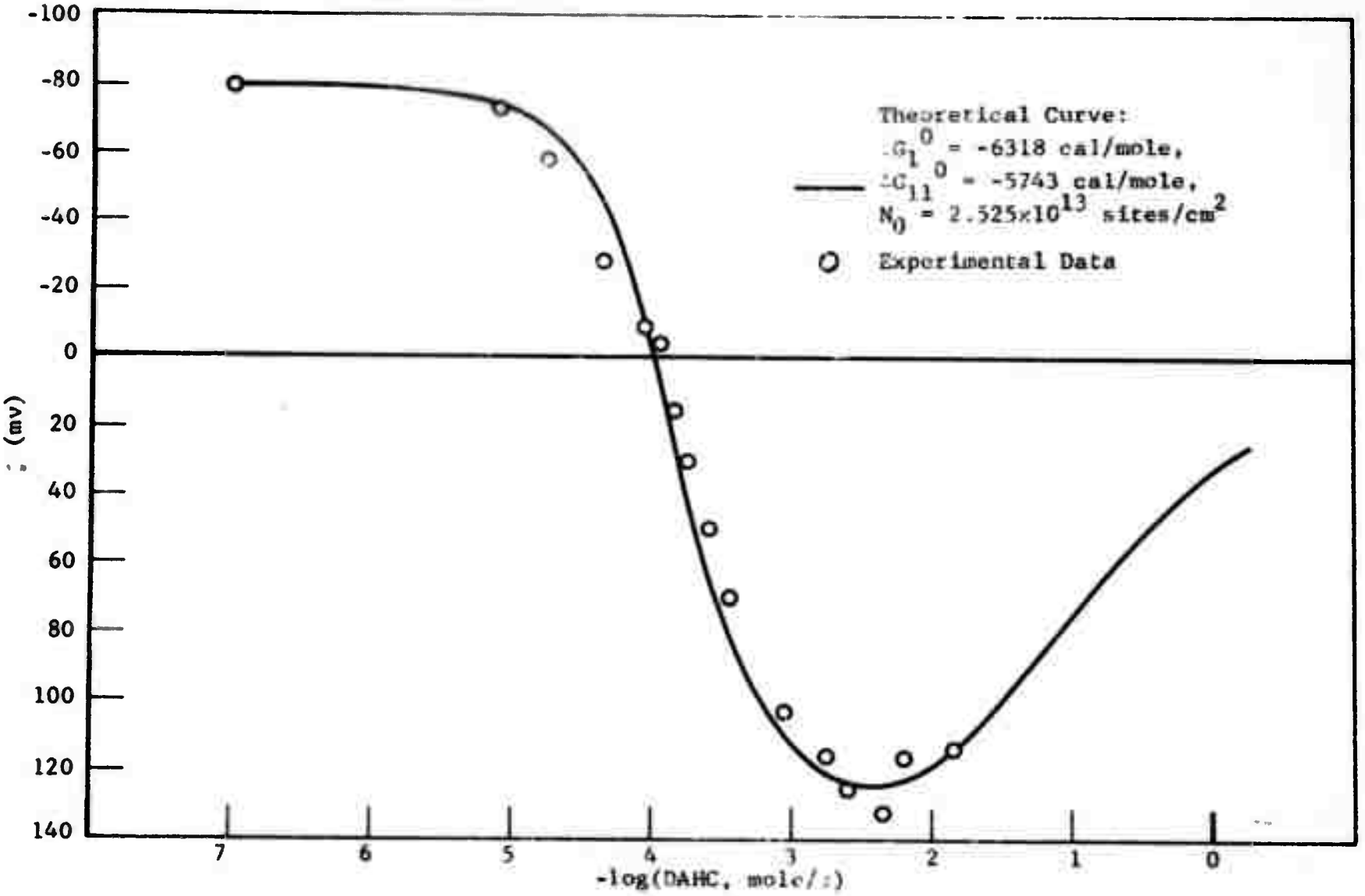

Figure 12

ZETA POTENTIAL VERSUS CONCENTRATION FOR COLLOIDAL AgI IN THE PRESENCE OF DODECYLAMINE HYDROCHLORIDE (DAHC)

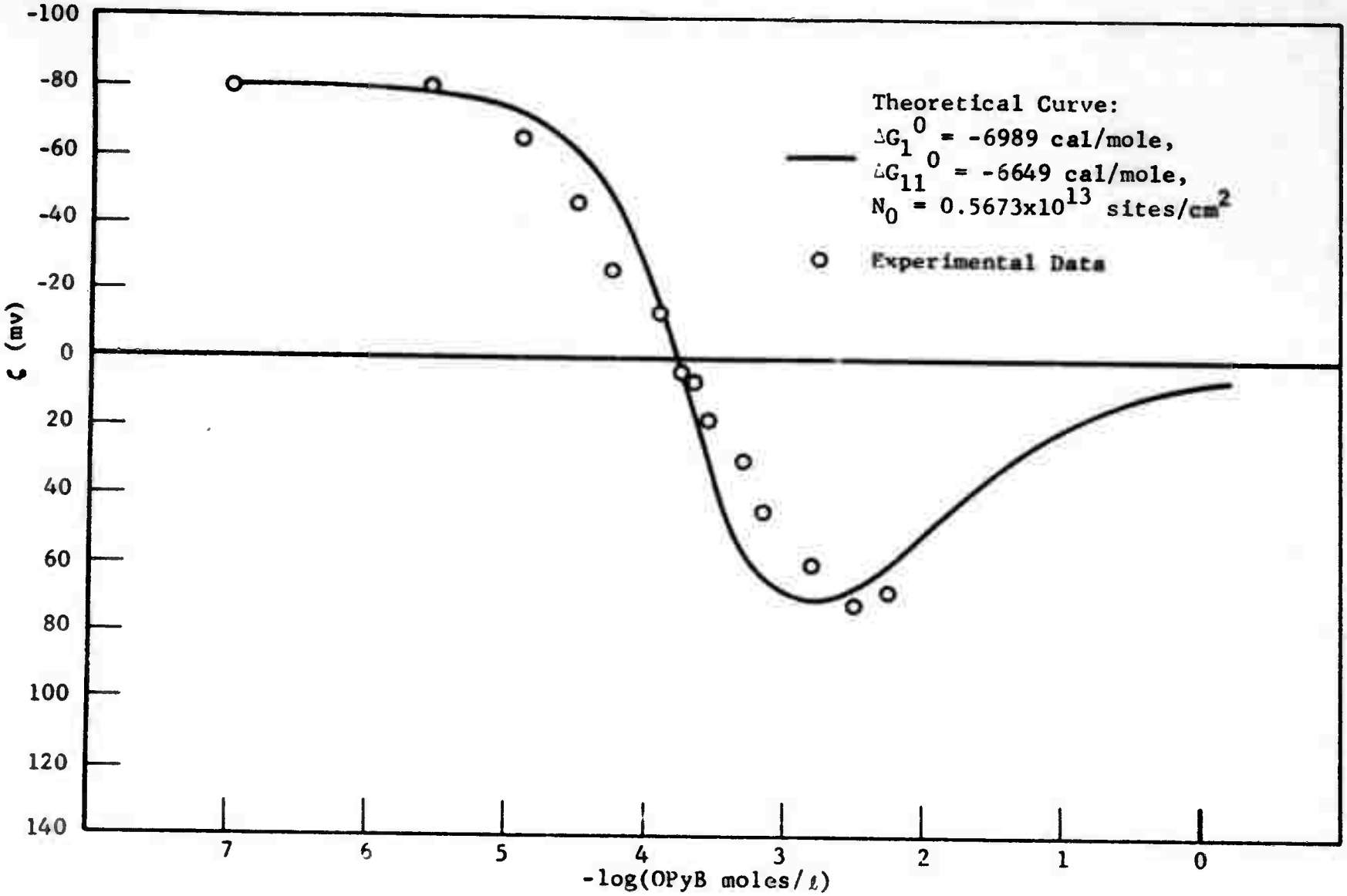

Figure 13

ZETA POTENTIAL VERSUS CONCENTRATION FOR COLLOIDAL AgI IN THE PRESENCE OF OCTYLPYRIDINIUM BROMIDE (OpyB)

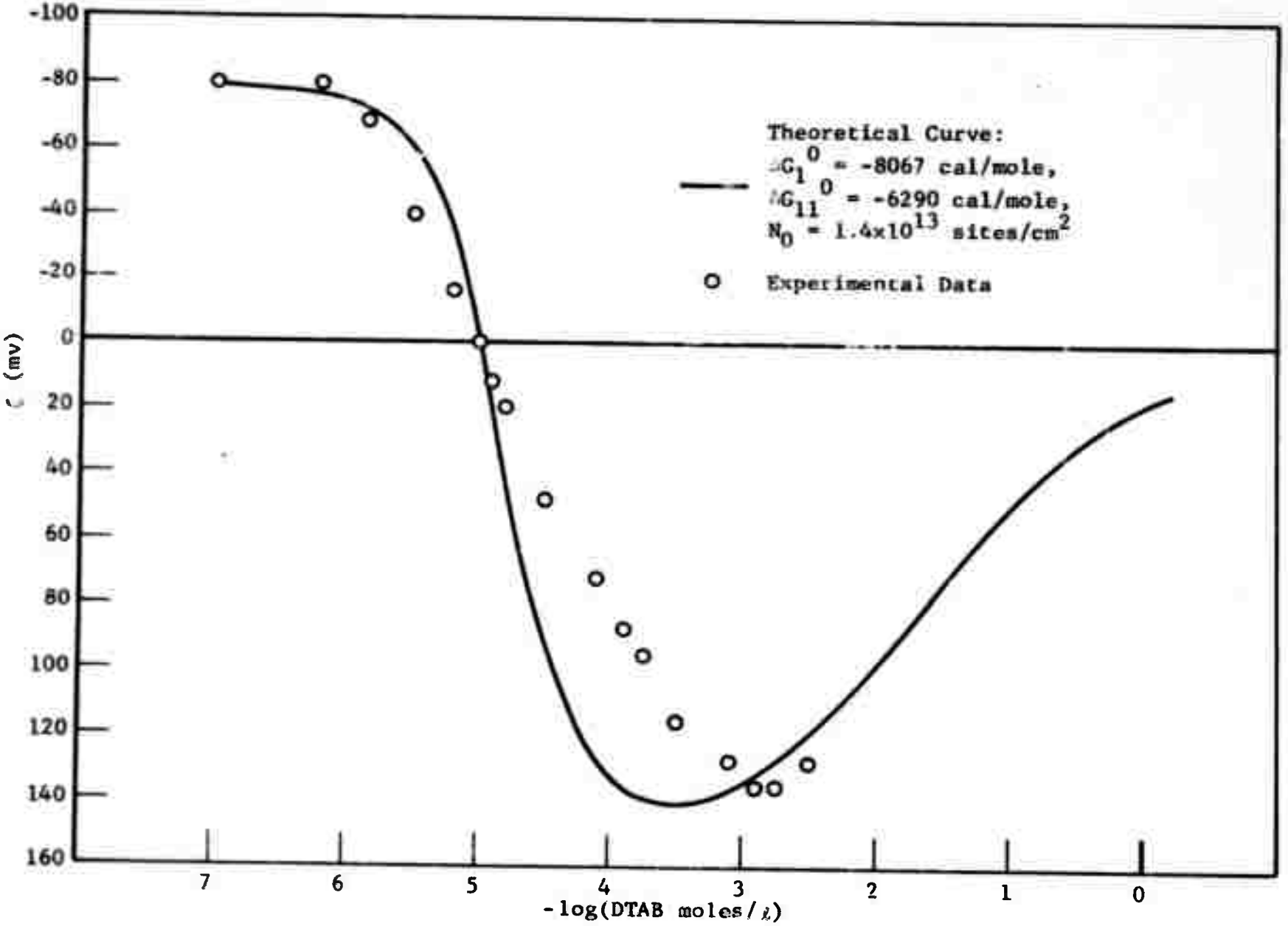

Figure 14

ZETA POTENTIAL VERSUS CONCENTRATION FOR COLLOIDAL AgI IN THE PRESENCE OF DODECYLTRIMETHYL-AMMONIUM BROMIDE (DTAB)

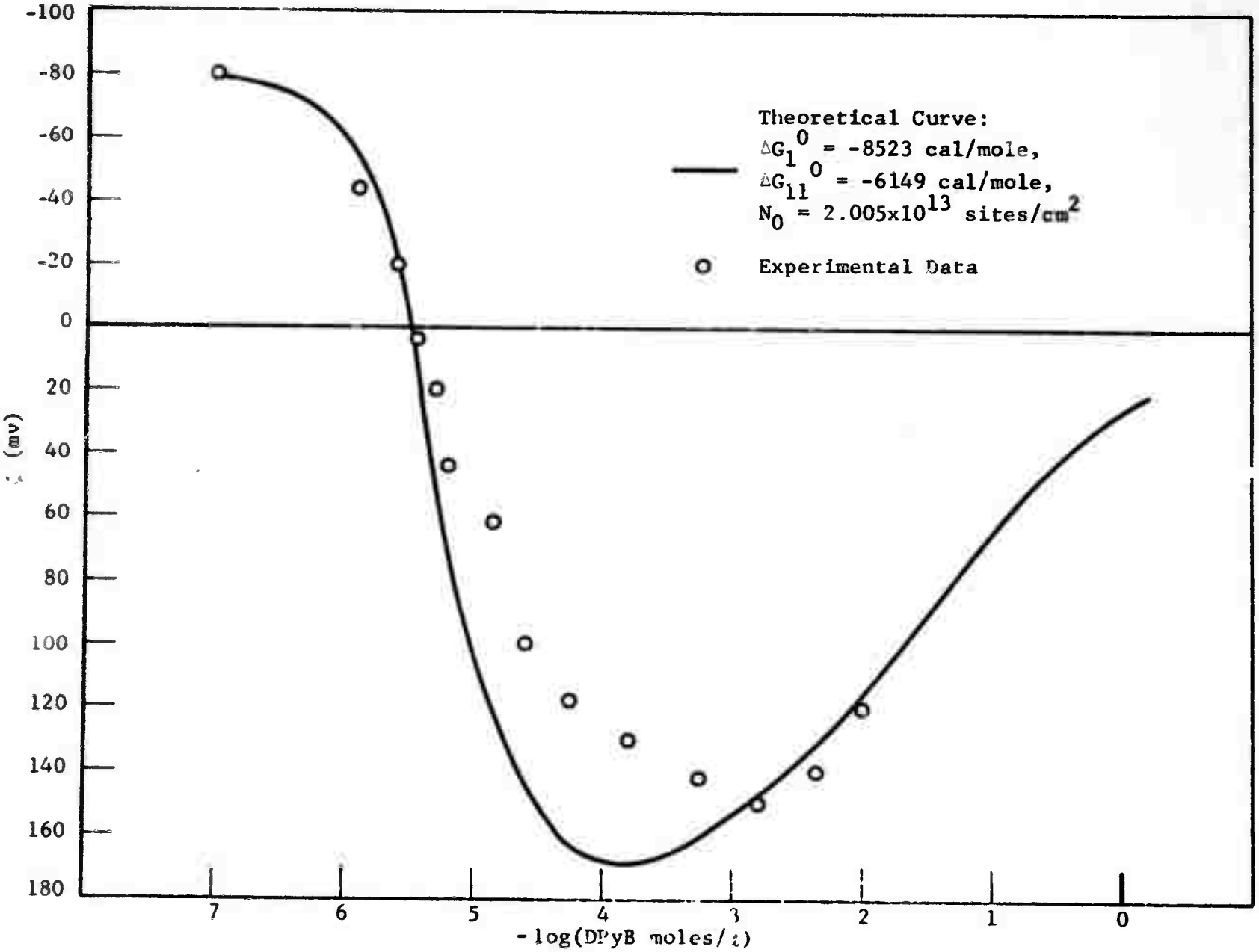

Figure 15

ZETA POTENTIAL VERSUS CONCENTRATION FOR COLLOIDAL AgI IN THE PRESENCE OF DODECYLPYRIDINIUM BROMIDE (DPyB)

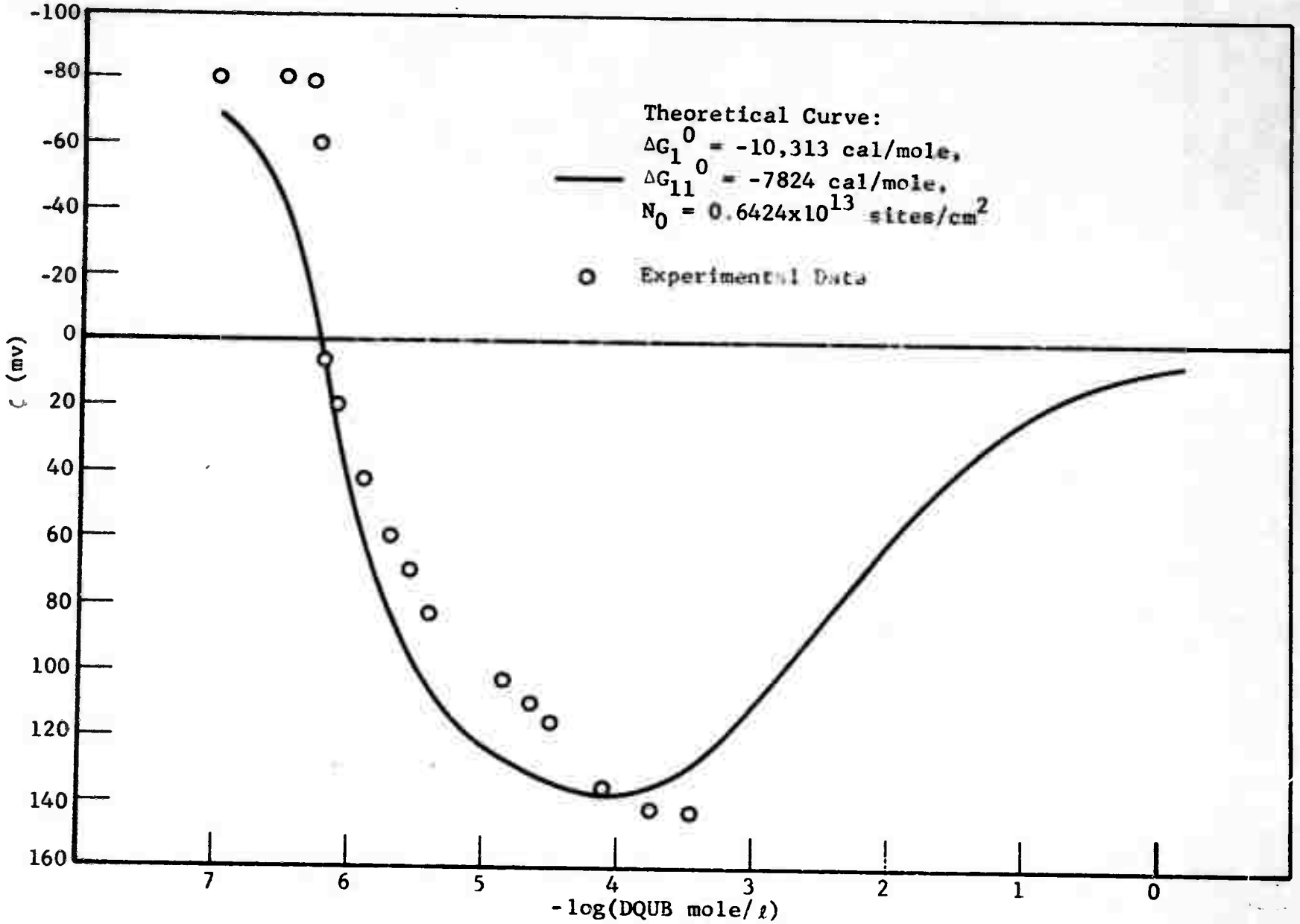

Figure 16

ZETA POTENTIAL VERSUS CONCENTRATION FOR COLLOIDAL AgI IN THE PRESENCE OF DODECYLQUINOLINIUM BROMIDE (DQUB)

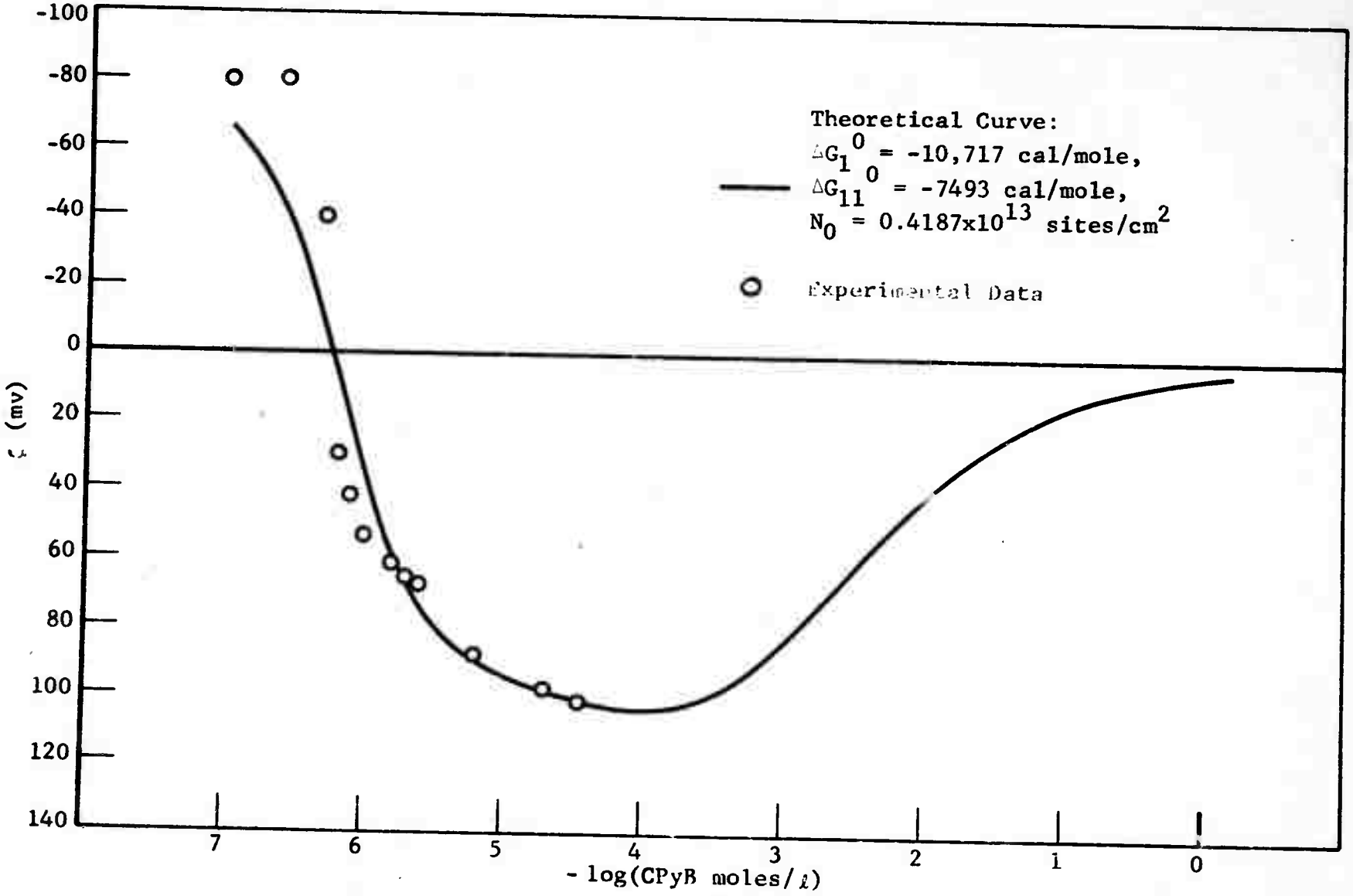

Figure 17

ZETA POTENTIAL VERSUS CONCENTRATION FOR COLLOIDAL AgI IN THE PRESENCE OF CETYLPYRIDINIUM BROMIDE (CPyB)

constant and thus is adsorbed into the parameters during regression. At polyelectrolytic concentration above 10^{-3} M, ψ_{0S} and ψ_{0P} become identical because $\kappa a \gg 1$. Therefore, good agreement between theory and data is expected in the concentration range 10^{-5} M > c > 10^{-5} M as found. However, in the range 10^{-5} M < c < 10^{-3} M, κa will vary and also be on the order of unity. As a result, it is seen from Equation 70 that the assumption of a planar surface will overestimate the true surface potential.

Therefore, it may be concluded that the theory presented for the development of surface charge due to adsorption is both conceptually and quantitatively correct.

8.2 Comparison of Surface Dissociation Theory with Experimental Data

The theory presented for the development of surface charge due to the dissociation of surface groups will now be compared with experimental data. The study of Modi and Fuerstenau (1957) will be used for this purpose. They measured the zeta potential of alumina in aqueous solutions at various pH values and salt concentrations by the streaming potential method in a packed bed. The size of the particles was 48/65 mesh.

Since the particle size is on the order of microns, the value of κa is much greater than one so that the particles may be treated as planar surfaces. Thus, the surface charge was calculated from the zeta potential measurements according to Equation 35. Also, since the zero point charge occurs at pH 9.4, it was assumed that the surface consisted only of $Al(OH)_3$ groups.

As a result, the adsorption isotherm given by Equation 65 with $N_P = 0$ was used to predict the surface charge. The values of the parameters N_0, K_{01}, K_{02}, K_{03}, K_{04} were obtained by regression analysis performed by the computer program to give

$$N_0 = 1.557 \times 10^{13} \text{ sites/cm}^2$$

$$K_{01} = 1.0$$

$$K_{02} = 0.02138$$

$$K_{03} = 4.678 \times 10^{-6}$$

$$K_{04} = 3.613 \times 10^{-11}$$

It is noted that the number of sites is in agreement with the common fact that it should be on the order of 10^{13} sites/cm^2. Also, the values of the equilibrium constants decrease in the order $K_{01}, \ldots\ldots, K_{04}$ as predicted and are of reasonable magnitudes. It was found that calculations were insensitive to K_{01} which combined with its large value indicates that Al^{+3} was not formed on the surface. This makes sense because it is not expected that the bare metal would be exposed.

The surface charge predicted by Equation 65 as a function of pH and ionic strength is compared with experimental data in Figure 18. Similar comparisons are given in Figure 19 where surface charge is plotted against pH and in Figure 20 where surface charge is plotted against salt concentration for various pH values. From these graphs, it is seen that the theoretical and experimental results are in good agreement at high and low pH values but that there is somewhat poor agreement aroung pH 7. Also, the isoelectric point is incorrectly predicted to be pH 7.8 instead of the experimental value of pH 9.4. However, these discrepancies can probably be accounted for by hypothesizing that a small fraction of the $Al(OH)_3$ surface groups are really AlO·OH groups. It is expected that such a surface would allow the calculated isoelectric point to occur at a higher pH. This projection is based on numerical computations performed during the course of the regression analysis.

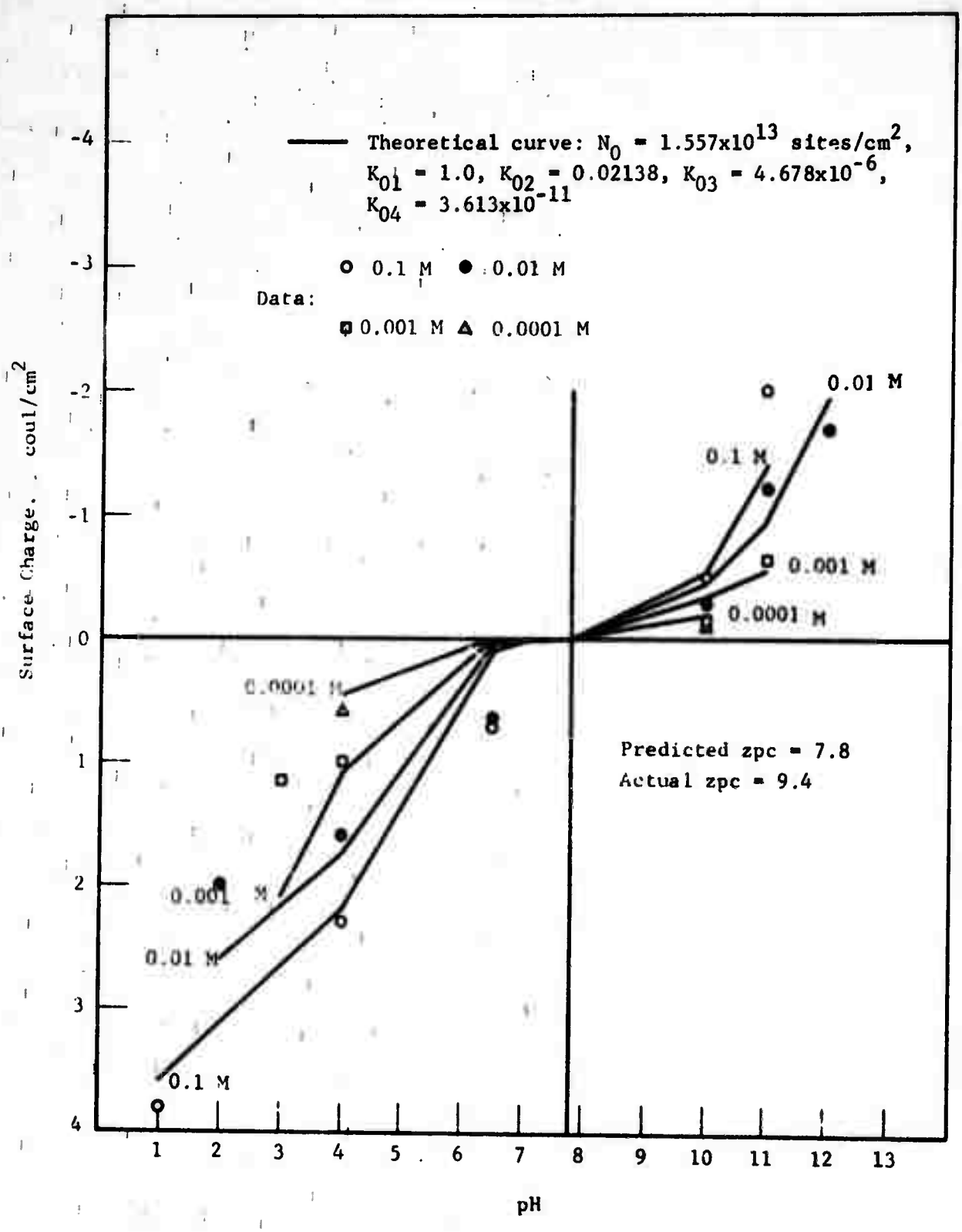

Figure 18

SURFACE CHARGE OF ALUMINA VERSUS pH AND IONIC STRENGTH

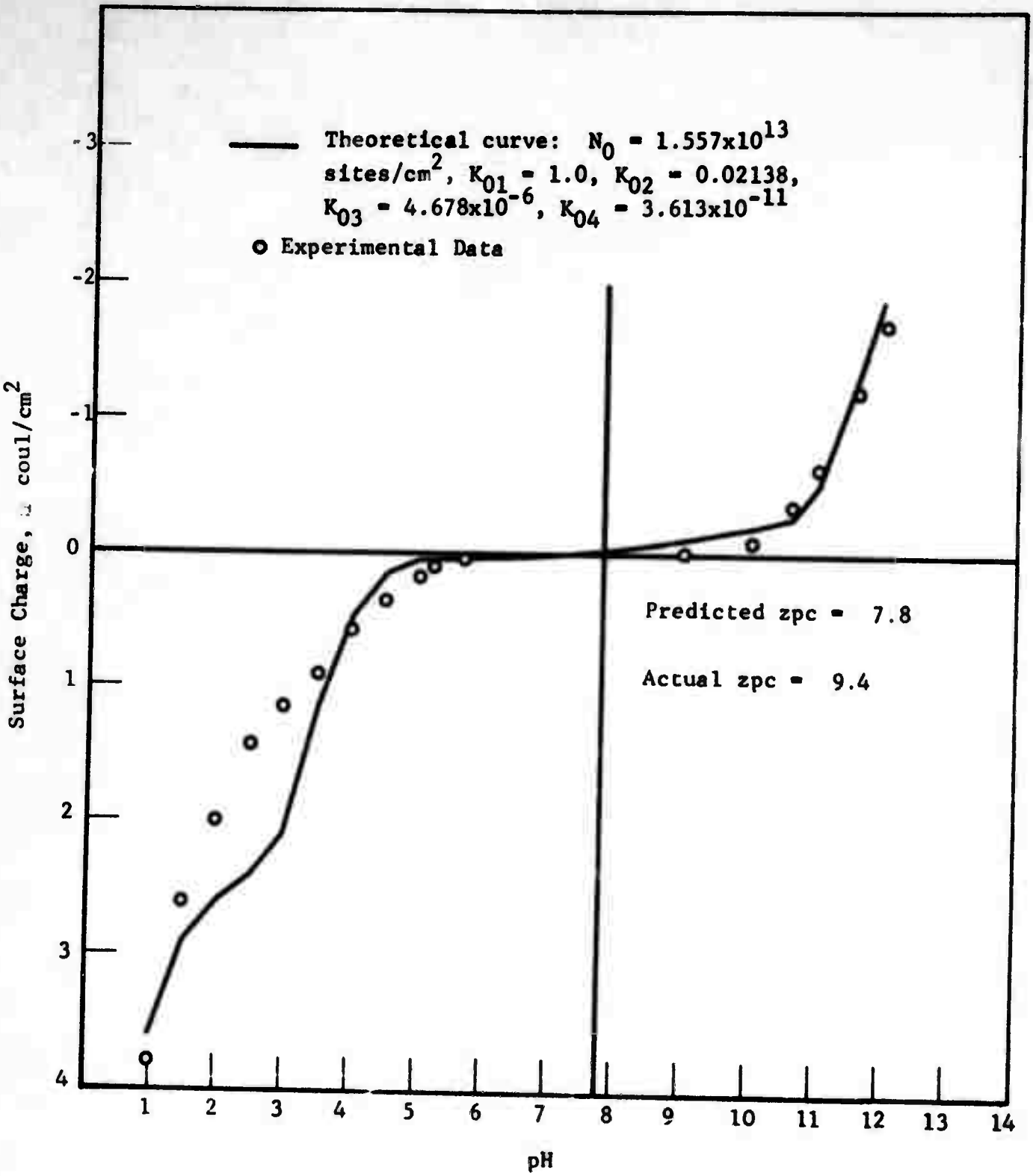

Figure 19

SURFACE CHARGE OF ALUMINA VERSUS pH

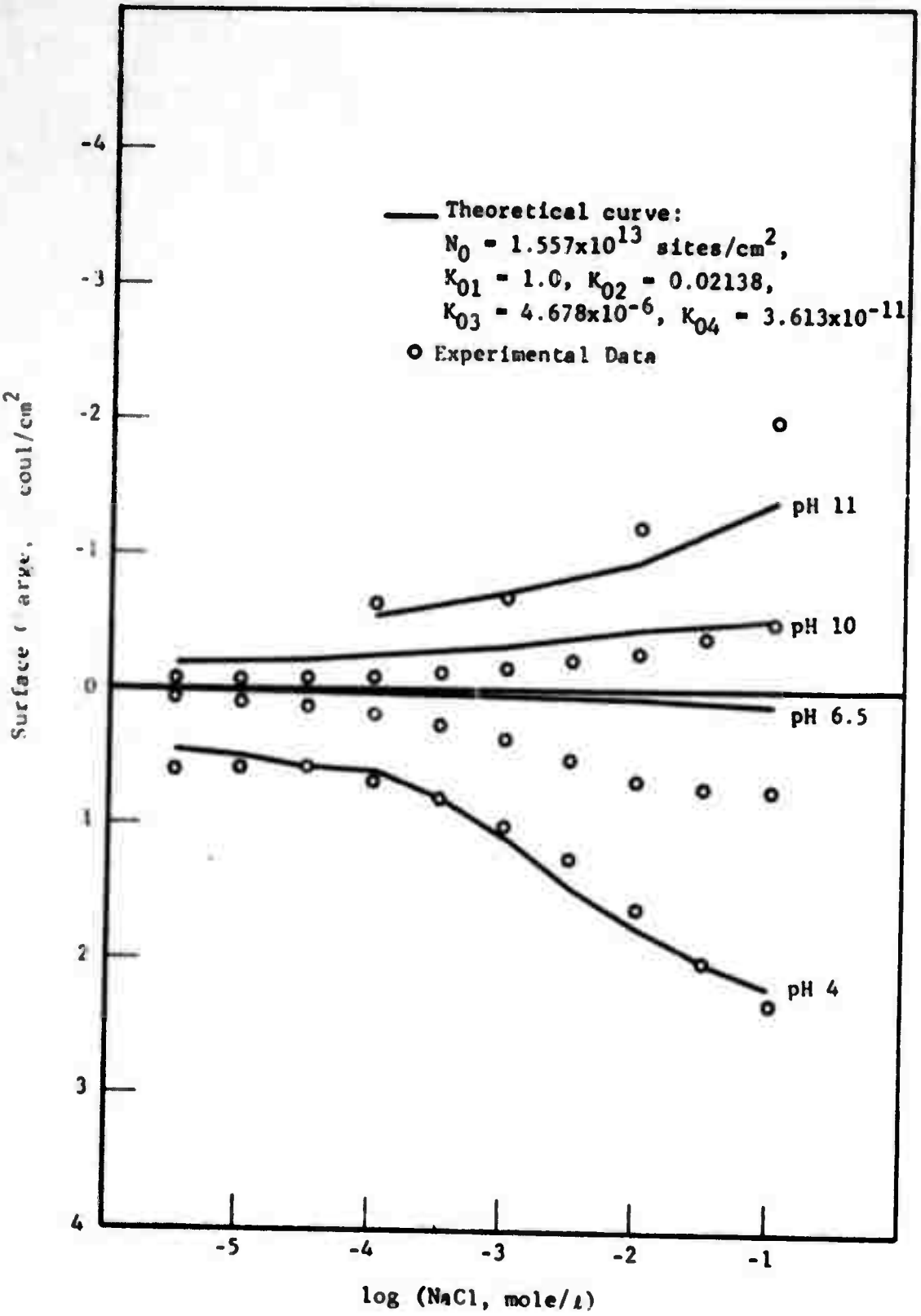

Figure 20

SURFACE CHARGE OF ALUMINA VERSUS CONCENTRATION OF NaCl IN VARIOUS pH SOLUTIONS

Although there is not complete agreement between theory and data, there is sufficient agreement to substantiate the concept of surface dissociation as a charging mechanism for alumina and the basic mathematical model.

9. TOTAL ENERGY OF INTERACTION CURVES

9.1 van der Waals-London Attraction

As discussed in the literature review, the total interaction energy of two colloidal particles is given by the sum of the interaction energies due to van der Waals-London attractive forces and to electrical double-layer interaction.

The energy V_A of interaction between two spherical particles was considered in detail in this review, and it was shown that for small separation distances

$$V_A = \frac{- Aa_1a_2}{6(a_1 + a_2)H_0} \tag{71}$$

where

A is the Hamaker constant

a_1, a_2 are the radii of the particles

H_0 is the shortest distance between their surfaces.

The effects of retardation and adsorbed layers were also considered.

The theory for the van der Waals force is well established and complete so that no improvements or modifications were necessary. For this reason, there will be no further discussion of this subject, and the reader is referred to the literature review for details. However, in the case of electrical double-layer interaction, it was necessary to extend the present theory as given on the following pages.

9.2 Electrical Double-Layer Repulsion

Although there have been detailed calculations carried out by several investigators (Kruyt, 1952; Devereux and de Bruyn, 1963; Honig and Mul, 1971) of the energy of interaction between

the electrical double layers associated with two particles, the results of these studies are given in tabular form rather than as equations because graphical or numerical integrations were performed. However, since this interaction energy is to be used later in this project in calculations which involve integration and the solution of differential equations, such solutions will make these further operations extremely unwielding. Thus, there is a distinct need for equations which can approximately describe this interaction. Unfortunately, the two most promising ones available are restricted to the interaction of particles with the same surface potential (Honig and Mul, 1971) while for particles with different potentials to the case where the potentials do not exceed an absolute value of 50 mv (Hogg et al., 1966). In this section, the limits of these approximate equations will be extended.

9.2.1 Approximation for Large and Moderate Particle Separation

The basis of this method was originally worked out by Verwey and Overbeek (1948) for two flat plates with identical surface potentials. When the two surfaces are relatively far apart, there is small interaction so that the potential between them can be obtained by adding the potentials due to two isolated surfaces. From this, the interaction between spheres is then obtained by Derjaguin's method which considers the spherical surface to be made up of flat rings. Justification for this procedure is that for the case of identical surface potentials, results of this method are in good agreement with exact numerical calculations (Honig and Mul, 1971).

An expression for the potential of an isolated flat plate is obtained from the Poisson Boltzmann equation (Equation 31) written in the form (Verwey and Overbeek, 1948)

$$\frac{d^2y}{d\xi^2} = \text{Sinh}y \tag{72}$$

where

$$y = \frac{ze\psi}{kT}$$

$$\xi = \kappa x$$

subject to

$$y = y_0 \text{ at } \xi = 0 \quad \text{and} \quad y = \frac{dy}{d\xi} = 0 \text{ as } \xi \to \infty$$

The hyperbolic sine term is a result of assuming that all the electrolytes in solution are of valency z. This simplication is permissible because ions with the same charge of the surface are not important (Kruyt, 1952).

The solution of Equation 72 is

$$e^{y/2} = \frac{e^{y_0/2} + 1 + (e^{y_0/2} - 1)e^{-\xi}}{e^{y_0/2} + 1 - (e^{y_0/2} - 1)e^{-\xi}} \tag{73}$$

Writing Equation 73 as

$$y = 2 \ln \frac{1 + \nu e^{-\xi}}{1 - \nu e^{-\xi}} \tag{74}$$

where

$$\nu = \frac{e^{y_0/2} - 1}{e^{y_0/2} + 1}$$

It is seen that sufficiently far away from the surface such that $\xi >> 1$ Equation 74 simplifies to

$$y \approx 2 \ln(1 + 2\nu e^{-\xi})$$

$$\approx 4\nu e^{-\xi} \tag{75}$$

as a result of expansion in series of the logarithmic term. It has been shown that Equation 75 is a very good approximation for $\zeta \geq 1$ (Verwey and Overbeek, 1948).

If the two plates are located a distance 2d apart, then from Equation 75 the contribution of Plate 1 at x = 0 to the potential in the solution is

$$y_1 = 4\nu_1 e^{-\zeta} \tag{76}$$

and that of Plate 2 at x = 2d

$$y_2 = 4\nu_2 e^{(\zeta - 2\kappa d)} \tag{77}$$

Thus, adding Equations 76 and 77, the potential between the plates is

$$y = 4\left[\nu_1 e^{-\zeta} + \nu_2 e^{(\zeta - 2\kappa d)}\right] \tag{78}$$

The force and thereby the interaction energy between the plates are obtained by following the method by Verwey and Overbeek (1948). It is assumed that the plates are kept apart by a pressure P and the liquid between them is in contact with a large reservoir at potential zero and pressure p_0. A force balance on any point in the liquid between the plates gives the force F at that point as

$$dF = dp - \rho E dx = dp + \rho d\psi = 0 \tag{79}$$

Introducing the Poisson equation, Equation 79 becomes

$$\frac{dF}{dx} = \frac{dp}{dx} - \frac{\varepsilon}{4\pi}\frac{d^2\psi}{dx^2}\frac{d\psi}{dx} = 0$$

Integration yields

$$F = p - \frac{\varepsilon}{8\pi}\left(\frac{d\psi}{dx}\right)^2 = \text{constant} \tag{80}$$

The constant of integration is given by the pressure where $\frac{d\psi}{dx} = 0$. This point x_m is found by taking the derivative of Equation 78 with respect to ξ and setting it equal to zero.

$$\frac{dy}{d\xi} = 4\left[- \nu_1 e^{-\xi_m} + \nu_2 e^{\xi_m - 2\kappa d} \right] = 0$$

$$\frac{\nu_1}{\nu_2} = e^{2\kappa (x_m - d)}$$

$$x_m = d + \frac{1}{2\kappa} \ln \frac{\nu_1}{\nu_2} \tag{81}$$

or

$$\xi_m = \kappa d + \frac{1}{2} \ln \frac{\nu_1}{\nu_2} = \kappa d + \Delta \tag{82}$$

where

$$\Delta = \frac{1}{2} \ln \frac{\nu_1}{\nu_2}$$

The force driving the plates apart due to the double interaction is the force relative to the reservoir pressure and is obtained from Equation 79 as

$$P = F - p_\infty = p_m - p_0 = \int_{\psi=0}^{\psi=\psi_m} dp = - \int_0^{\psi_m} \rho d\psi \tag{83}$$

Writing the charge density in accordance with Equation 72 as

$$\rho = - 2zen_0 \operatorname{Sinh} \frac{ze\psi}{kT}$$

and substituting it into Equation 83,

$$P = 2n_0 kT \left[\cosh \left(\frac{ze\psi_m}{kT} \right) - 1 \right] \tag{84}$$

Since weak interaction between the particles has been assumed, it is sufficient to use the first-order term in the Taylor expansion of Equation 84 about $\psi_m = 0$ as given by

$$P = n_0 kT \left(\frac{ze\psi_m}{kT} \right)^2 = n_0 kT y_m^2 \tag{85}$$

Substitution of Equation 78 into Equation 85 yields

$$P = n_0 kT y_m^2 = 16 \left[\nu_1^2 e^{-2\xi_m} + \nu_2^2 e^{2(\xi_m - 2\kappa d)} + 2\nu_1\nu_2 e^{-2\kappa d} \right] n_0 kT$$

$$= 16 \left[\nu_1^2 e^{-2\Delta} + \nu_2^2 e^{2\Delta} + 2\nu_1\nu_2 \right] n_0 kT e^{-2\kappa d} \tag{86}$$

The energy of interaction V_R is determined from the relation

$$V_R = - \int_{\infty}^{2d} P(2d)\, d(2d)$$

which upon substitution of Equation 86 gives

$$V_R = - 16 \left[\nu_1^2 e^{-2\Delta} + \nu_2^2 e^{2\Delta} + 2\nu_1\nu_2 \right] n_0 kT \int_{\infty}^{2d} e^{-\kappa t} dt$$

$$= 16 \left[\nu_1^2 e^{-2\Delta} + \nu_2^2 e^{2\Delta} + 2\nu_1\nu_2 \right] \frac{n_0 kT}{\kappa} e^{-2\kappa d} \tag{87}$$

From this result, it is now possible to calculate the interaction between spherical particles by means of Derjaguin's method (Verwey and Overbeek, 1948; Kruyt, 1952). If the thickness of the double layers is small relative to the radius of the particles ($\kappa a > 5$), the double layer interaction between spherical particles can be considered to consist of contributions from differential parallel rings as shown in Figure 21. Treating each pair of rings independently as two flat plates, the energy of interaction between two spherical particles can be written as

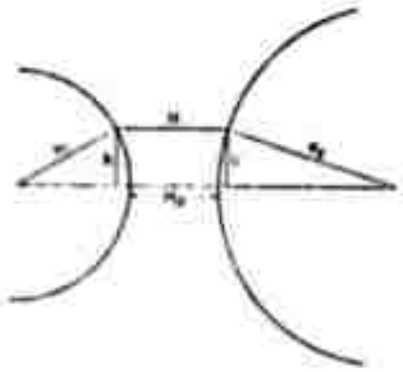

Figure 21

GEOMETRICAL CONSTRUCTION USED IN THE CALCULATION OF THE INTERACTION BETWEEN TWO DISSIMILAR SPHERICAL PARTICLES, RADII a_1 AND a_2 FROM THE INTERACTION OF TWO INFINITE FLAT PLATES
(from Hogg et al., 1966)

$$V_R = \int_0^\infty 2\pi h V_{plate} dh \qquad (88)$$

From the geometry of Figure 21

$$H = a_1 + a_2 - \sqrt{a_1^2 - h^2} - \sqrt{a_2^2 - h^2} + H_0 \qquad (89)$$

Differentiation of Equation 89 with respect to h yields

$$dH = \left[\frac{1}{a_1\sqrt{1 - h^2/a_1^2}} + \frac{1}{a_2\sqrt{1 - h^2/a_2^2}} \right] hdh$$

which simplifies to

$$hdh \approx \left(\frac{a_1 a_2}{a_1 + a_2} \right) dH \qquad (90)$$

under the reasonable assumption $h \ll a_1$ and $h \ll a_2$.

Substituting Equation 90 into Equation 88

$$V_R = \frac{2\pi a_1 a_2}{a_1 + a_2} \int_{H_0}^{\infty} V_{Plate}(H)\,dH \tag{91}$$

Finally, substituting Equation 87 into Equation 91 and carrying out the integration with $H = 2d$

$$V_R = \frac{32\pi a_1 a_2}{a_1 + a_2} \left[\nu_1^2 e^{-2\Delta} + \nu_2^2 e^{2\Delta} + 2\nu_1\nu_2 \right] \frac{n_0 kT}{\kappa^2} e^{-\kappa H_0} \tag{92}$$

For the special case where $a_1 = a_2 = a$, Equation 92 reduces to

$$V_R = \frac{64\pi a \nu^2 n_0 kT}{\kappa^2} e^{-\kappa H_0} \tag{93}$$

which has been extensively compared by Honig and Mul (1971) and found to be in good agreement with exact numerical calculations for $\kappa H_0 \geq 1$. Since van der Waal's forces start to dominate around $\kappa H_0 = 1$, Equation 92 is a very useful approximation.

9.2.2 Approximation for Small Particle Separation

The rationale for this method is that for small separation distances between two particles the potential in solution will not decrease a great amount from that at the surface. Thus, one can linearize the Poisson Boltzmann equation by expanding the charge density about the value of the surface potential. The procedure from this point on is similar to that used in obtaining the previous approximation. The interaction between two flat plates is found first, and then Derjaguin's method is used to calculate the interaction between two spherical particles. Hogg, Healy, and Fuerstenau (1966) have carried out this method for the case where the charge density was expanded about a potential of zero. Their results simplified the calculations for the present task.

It has been commonly assumed in the literature for mathematical convenience that as two particles approach each other their surface potentials do not change, and as a result, their surface charges diminish. This implies that adsorption equilibrium is rapidly established. However, it is doubtful that this is true, and a more appropriate assumption is constancy of the surface charge although the actual case lies somewhere in between these limiting cases. This implies slow desorption which seems more reasonable in light of the short particle contact times involved due to Brownian motion. Unfortunately, this assumption complicates the mathematics somewhat. For this reason, the fact that the results of either assumption do not differ significantly will be used so that constant surface potentials can be assumed. This has been shown to be true by Honig and Mul ('1971) who performed exact numerical calculations for the interaction energy at both constant surface potential and charge. Only at very small separation distances where the van der Waals forces would dominate are the results in disagreement.

The first step in the derivation is to linearize the Poisson-Boltzmann equation

$$\nabla^2 \psi = -\frac{4\pi}{\epsilon} \sum_i z_i e n_{i0} e^{-z_i e \psi / kT} \qquad (94)$$

Expanding in series the exponential terms about some reference potential ψ_R such as the average of the potentials of the two particles and retaining only the linear terms, Equation 94 becomes

$$\nabla^2 \psi = -\frac{4\pi}{\epsilon} \rho_R + \hat{\kappa}^2 (\psi - \psi_R) \qquad (95)$$

where

$$\rho_R = \sum_i z_i e n_{i0} e^{-z_i e \psi_R / kT}$$

$$\hat{\kappa}^2 = \frac{4\pi e^2}{\epsilon kT} \sum_i z_i^2 n_{i0} e^{-z_i e \psi_R / kT}$$

Equation 95 is to be solved for two flat plates subject to the boundary conditions

$$\psi = \psi_{01} \qquad \text{at} \qquad z = 0$$

$$\psi = \psi_{02} \qquad \text{at} \qquad x = 2d$$

If a change of variables is made

$$\hat{\psi} = \psi - \psi_R - \frac{4\pi}{\hat{\kappa}^2 \epsilon} \rho_R$$

or

$$\psi = \hat{\psi} + \psi_R + \frac{4\pi}{\epsilon \hat{\kappa}^2} \rho_R \tag{96}$$

then the problem to be solved is

$$\frac{d^2 \hat{\psi}}{dx^2} = \hat{\kappa}^2 \hat{\psi} \tag{97}$$

subject to

$$\hat{\psi} = \psi_{01} - \psi_R - \frac{4\pi\rho_R}{\epsilon\hat{\kappa}^2} = \hat{\psi}_{01} \qquad \text{at} \qquad x = 0$$

$$\hat{\psi} = \psi_{02} - \psi_R - \frac{4\pi\rho_R}{\epsilon\hat{\kappa}^2} = \psi_{02} \qquad \text{at} \qquad x = 2d$$

The solution is

$$\hat{\psi} = \hat{\psi}_{01} \cosh \hat{\kappa} x + \left[\frac{\hat{\psi}_{02} - \hat{\psi}_{01} \cosh 2\hat{\kappa} d}{\text{Sinh } 2\hat{\kappa} d} \right] \text{Sinh} \hat{\kappa} x \tag{98}$$

The surface charge is calculated from the relation

$$q = -\frac{\epsilon}{4\pi}\left(\frac{d\psi}{dx}\right)_{surface}$$

which was derived earlier and yields the result

$$q_1 = -\frac{\epsilon\hat{\kappa}}{4\pi}\left[\hat{\psi}_{02}\ \mathrm{cosech}(2\hat{\kappa}d) - \psi_{01}\coth(2\hat{\kappa}d)\right] \qquad (99)$$

$$q_2 = -\frac{\epsilon\hat{\kappa}}{4\pi}\left[-\hat{\psi}_{02}\coth(2\hat{\kappa}d) + \psi_{01}\ \mathrm{cosech}(2\hat{\kappa}d)\right] \qquad (100)$$

Since the surface charge and potential are linearly related, the free energy G can be determined from

$$G = -\int_0^{\psi_0} q(\psi)\,d\psi$$

$$G = -\frac{1}{2}\left[q_1\psi_{01} + q_2\psi_{02}\right]$$

with the result that the interaction energy V_{Plate} is

$$V_{Plate} = G_{2d} - G_{\infty}$$

$$= \frac{\epsilon\hat{\kappa}}{8\pi}\left\{\left[\psi_{01}^2 + \psi_{02}^2 - \Delta\psi_R\left(\psi_{01} + \psi_{02}\right)\right]\left[1 - \coth(2\hat{\kappa}d)\right] + \left[2\psi_{01}\psi_{02} - \Delta\psi_R\left(\psi_{01} + \psi_{02}\right)\right]\ \mathrm{cosech}(2\hat{\kappa}d)\right\} \qquad (101)$$

where

$$\Delta\psi_R = \psi_R + \frac{4\pi}{\epsilon\hat{\kappa}^2}\rho_R$$

Then, using Derjaguin's method, the interaction energy for two spherical particles is

$$V_R = \frac{2\pi a_1 a_2}{a_1 + a_2} \int_{2d}^{\infty} V_{Plate}(2d)\,d(2d)$$

$$= \frac{\epsilon a_1 a_2}{4(a_1 + a_2)} \left[\psi_{01}^2 + \psi_{02}^2 - \Delta\psi_R(\psi_{01} + \psi_{02}) \right]$$

$$\cdot \left\{ \frac{\left[2\psi_{01}\psi_{02} - \Delta\psi_R(\psi_{01} + \psi_{02}) \right]}{\psi_{01}^2 + \psi_{02}^2 - \Delta\psi_R(\psi_{01} + \psi_{02})} \ln\left(\frac{1 + \epsilon^{-\hat{\kappa}H_0}}{1 - \epsilon^{-\hat{\kappa}H_0}} \right) \right.$$

$$\left. + \ln\left(1 - \epsilon^{-2\hat{\kappa}H_0} \right) \right\} \qquad (102)$$

For $\psi_R = 0$ and thus $\Delta\psi_R = 0$ and $\hat{\kappa} = \kappa$, Equation 102 simplifies to that obtained by Hogg et al. (1966) which they showed to be in agreement with exact numerical results for $\psi_0 \leq 60$ mv. Thus, it is expected that Equation 102 will be a good approximation for the case where the separation distance is such that the potential in solution does not vary more than 60 mv from the surface potential. This situation should occur for at least $\kappa H_0 < 1$ if not a greater value. The reasoning behind this is that since the double layer thickness of an isolated particle is $1/\kappa$, $\kappa H_0 = 1$ suggests that potentials at positions no greater than half a double layer thickness are being considered. At a distance of half a double layer away from the surface, the Debye-Hückel approximation $\psi = \psi_0 e^{-\kappa x}$ shows that the potential has only diminished to 60 percent of that at the surface. Thus, for a maximum surface potential of 150 mv, the potential only reduces to 90 mv so that the change is within 60 mv. Therefore, since Equation 92 is valid for $\kappa H_0 \geq 1$ and Equation 102 for $\kappa H_0 \leq 1$, these two equations together provide a good representation for the entire energy of interaction curve for two spherical particles.

10. CONCLUSIONS AND SUMMARY

It has been shown that the Gouy-Stern-Grahame model is inadequate for explaining the observed dependence of the zeta potential and surface charge on ionic strength, surfactant concentration and pH. It was necessary to explain two common types of experimental data: (1) zeta potential versus concentration and (2) surface charge versus ionic strength versus pH. It was shown that these phenomena are governed by competing phenomena (1) adsorption of ions from solution, (2) dissociation of surface groups due to chemical surface reactions, and (3) the thickness of the electrical double layer due to counter ions.

In the case of adsorption, the following was found. At low concentration, the adsorption effect dominates, and the zeta potential increases in absolute value with increasing concentration. At high concentrations, the double layer thickness effect dominates, and the zeta potential approaches zero with increasing concentration. The zeta potential versus concentration curve can be predicted mathematicaly by using a multi-component adsorption isotherm in conjunction with a relationship between the zeta potential and surface charge. For single layer adsorption, Equation 15 is used for the isotherm while for multi-layer adsorption, Equation 22 is used. For planar surfaces, the zeta potential and surface charge are related through Equation 35 while for spherical surfaces, a computer program serves this purpose. When the species to be adsorbed undergoes hydroxo complex formation, it is necessary to calculate the concentration of the various complexes. For an externally added electrolyte, Equation 57 is used while for ions derived from the particle, Equation 59 is used. Then Equation 15 is used to compute the surface charge due to adsorption of the complexes. Predicted zeta potential versus concentration curves were shown to be in good agreement with experimental data in the literature for AgI sols in the presence of polyelectrolytes.

For the case of surface dissociation, the following was found. For metal oxides, the surface consists of hydroxides of varying degrees of hydration. The greater degree of hydration the higher is the pH at which the zero point charge occurs. Equation 65 is used to calculate the surface charge while Equation 69 gives the dependence of the equilibrium constants on the surface charge or zeta potential. The zeta potential and surface are related as described above. It was shown that this dependence of the equilibrium constants is the reason why the surface charge increases in absolute magnitude with increasing ionic strength. Predicted surface charge versus ionic strength versus pH curves were shown to be in good agreement with experimental data in the literature for alumina at various pH and NaCl solutions.

In order to predict the interaction of two particles when they approach each other, the theory of interaction energy curves was studied. It was found that the theory for van der Waals forces is sufficiently complete so that no improvements were necessary. However, in the case of the electrical forces due to double layer interaction, it was necessary to extend the present theory. Although exact numerical calculations have been performed, they are not convenient to use so that it was necessary to derive approximate analytical expressions. The entire interaction energy curve for spherical particles of arbitrary size and surface potential is described by Equation 102 for small separation distances ($\kappa a < 1$) and Equation 92 for moderate and large separation distances. These equations are in good agreement with the limited exact results.

When the attraction energy curve due to van der Waals-London forces and the repulsion energy curve due to double layer interaction are added together, the total interaction energy curve is obtained from which the stability of a colloidal system can be deduced.

REFERENCES

Bikerman, J. J., Phil. Mag., 33, 384 (1942).

Booth, F., J. Chem. Phys., 19, 391, 1327, 1615 (1951).

Brossett, C. et al., "Studies on the Hydrolysis of Metal Irons: XI, The Aluminum Ion Al^{+3}," Acta Chem. Scand., 8, 1917 (1954).

Devereux, O. F. and de Bruyn, P. L., Interactions of Plane-Parallel Double Layers, M.I.T. Press, Cambridge, Mass., 1963.

Fowler, R. H. and Guggenheim, E. A., Statistical Thermodynamics, Cambridge University Press, p. 426, 1965.

Freyberger, W. L. and de Bruyn, P. L., "The Electric Chemical Double Layer on Silver Sulfide," J. Phys. Chem., 61, 586 (1957).

Fuerstenau, D. W. and Modi, H. J., "Streaming Potentials of Corundum in Aqueous Organic Electrolyte Solutions," Electrochem. Soc., 106, 336 (1959).

Gaudin, A. M. and Fuerstenau, D. W., "Quartz Flotation with Anionic Collectors," Trans. AIME, 202, 66 (1955).

Hogg, R., Healy, T. W. and Fuerstenau, D. W., "Mutual Coagulation of Colloidal Dispersions," Trans. Faraday Soc., 62, 1638 (1966).

Honig, E. P. and Mul, P. M., "Tables and Equations of the Diffuse Double Layer Repulsion at Constant Potential and at Constant Charge," J. Coll. Sci., 36, 258 (1971).

Hsu, P. H. and Bates, T. F., Mineral Mag., 33, 749 (1964).

Hunter, R. J., "The Interpretation of Electrokinetic Potentials," J. Coll. & Interf. Sci., 22, 231 (1966).

Hunter, R. J. and Wright, H. J. L., "The Dependence of Electrokinetic Potential on Concentration of Electrolyte," J. Coll. & Interf. Sci., 37 (3), 564, Nov. 1971.

Kruyt, H. R., Colloid Science, Vol. 1, Elsevier Publ. Co., Amsterdam, 1952.

Lyklema, J. and Overbeek, J. Th. G., "On the Interpretation of Electrokinetic Potentials," J. Coll. Sci., 16, 501 (1961).

Matijevic, E. et al., "Detection of Ion Hydrolysis by Coagulation (III, Aluminum)," J. Phys. Chem., 65, 826 (1961).

Modi, H. J. and Fuerstenau, D. W., "Streaming Potential Studies on Corundum in Aqueous Solutions of Inorganic Electrolytes," J. Phys. Chem., 61, 640 (1957).

Moore, W. J., Physical Chemistry, Prentice-Hall Inc., Englewood Cliffs, N. J., p. 546, 1964.

Napper, D. H., "Colloid Stability," Ind. Eng. Chem. Prod. Res. Develop., 9 (4), 467 (1970).

O'Connor, D. J., Johansen, P. G. and Buchanan, A. S., "Electrokinetic Properties and Surface Reactions of Corundum," Faraday Soc. Trans., 52, 229 (1956).

Ottewill, R. H. and Watanabe, A., "Studies on the Mechanism of Coagulation. Part I. The Stability of Positive Silver Iodide Sols in the Presence of Anionic Surface Active Agents," Kolloid Zeit., 170 (1), 38 (1960).

Ottewill, R. H. and Watanabe, A., "Studies on the Mechanism of Coagulation. Part 2. The Electro Phoretic Behavior of Positive Silver Iodide Sols in the Presence of Anionic Surface Active Agents," Kolloid Zeit., 170 (2), 132 (1960).

Ottewill, R. H. and Watanabe, A., "Studies on the Mechanism of Coagulation. Part 3. The Formation of Positive Silver Iodide Sols in the Presence of Anionic Surface Active Agents," Kolloid Zeit., 171 (1), 33 (1960).

Ottewill, R. H. and Watanabe, A., "Studies on the Mechanism of Coagulation. Part 4. Some Considerations on the Coagulation of Sols of Small Spherical Particles under Conditions of Varying Ionic Strength and Surface Potential," Kolloid Zeit., 173 (1), 7 (1960).

Ottewill, R. H. and Watanabe, A., "Studies on the Mechanism of Coagulation. Part 5. The Coagulation of Sols of Silver Iodide Particles Coated with Tetradecyl Sulphate," Kolloid Zeit., 173 (2), 122 (1960).

Ottewill, R. H., Rastagi, M. C. and Watanabe, A., "The Stability of Hydrophobic Sols in the Presence of Surface-Active Agents," Faraday Soc. Trans., 56. Part 1. "Theoretical Treatment," p.854 (1960). Part 2. "The Stability of Silver Iodide Sols in the

Presence of Cationic Surface-Active Agents," (R. H. Ottewill and M. C. Rastagi), p. 866. Part 3. "An Examination by Microelectrophoresis of the Behavior of Silver Iodide Sols in the Presence of Cationic Surface-Active Agents," (R. H. Ottewill and M. C. Rastagi), p. 880.

Parfitt, G. D. (Ed.), Dispersion of Powders in Liquids, Elsevier Publ. Co., Amsterdam, 1969.

Parks, G. A., Equilibrium Concepts in Natural Water Systems "Aqueous Surface Chemistry of Oxides and Complex Oxide Minerals. Isoelectronic Point and Zero Point of Charge," Adv. in Chem. Ser., 67 (1967). Am. Chem. Soc., Wash., D.C.

Parks, G. A., "The Isoelectric Points of Solid Oxides, Solid Hydroxides, and Aqueous Hydroxo Complex Systems," Chem. Rev., 65, 177 (1965).

Parks, G. A. and de Bruyn, P. L., "The Zero Point of Charge of Oxides," J. Phys. Chem., 66, 967 (1962).

Parsons, R., Equilibrium Properties of Electrified Interphases in Modern Aspects of Electrochemistry, Vol. 1, 1954, Butterworth Publ., ed. J. O. . Bockris and B. E. Conway. Chapter 3, p. 103.

Rausch, W. V. and Bale, H. D., "Small Angle X-Ray Scattering from Hydrolyzed Aluminum Nitrate Solutions," J. Chem. Phys., 40, 3391 (1964).

Remy, H., Treatise on Inorganic Chemistry, Vol. 1, Elsevier Publ. Co., 1956, p. 353.

Riddick, T. M., Control of Colloid Stability Through Zeta Potential, Zeta-Meter Inc., 1968.

Robinson, M., Pask, J. A. and Fuerstenau, D. W., "Surface Charge of Alumina and Magnesia in Aqueous Media," J. Am. Cer. Soc., 47 (10), 518 (Oct. 1964).

Schlogl, R., Z. Phys. Chem., 202, 379 (1954).

Stumm, W. and Morgan, J. J., Aquatic Chemistry, an Introduction Emphasizing Chemical Equilibria in Natural Waters, Wiley-Interscience, New York 1970.

Stumm, W. and Morgan, J. J., "Chemical Aspects of Coagulation," J. AWWA, 54 (8), 971 (Aug. 1962).

Stumm, W. and O'Meila, C. R., "Stoichiometry of Coagulation," J. AWWA, 60 (5), 514 (May, 1968).

Sullivan, J. H., Jr. and Singley, J. E., "Reactions of Metal Ions in Dilute Aqueous Solution: Hydrolysis of Aluminum," J. AWWA, 60 (11), 1280 (Nov., 1968).

Tanford, C., Physical Chemistry of Macromolecules, Wiley & Sons Inc., New York, 1961.

Verwey, E. J. W. and Overbeek, J. Th. G., Theory of the Stability of Lyophobic Colloids, Elsevier Publ. Co., Amsterdam, 1948.

Yopps, J. A. and Fuerstenau, D. W., "The Zero Point of Charge of Alpha-Alumina," J. Coll. Sci. & Interf. Sci., 19 (1), 61 (Jan. 1964).